YGS Open File 2016-25

Geology of mid-Cretaceous volcanic rocks at Mount Nansen, central Yukon, and their relationship to the Dawson Range batholith

Marthe Klöcking and Logan Mills *Department of Earth Sciences, University of Cambridge, Cambridge, UK*

Jim Mortensen *Mineral Deposit Research Unit, University of British Columbia, Vancouver, BC*

and Charlie Roots† *Geological Survey of Canada, Whitehorse, Yukon*

Yukon Geological Survey

Yukon Energy, Mines and Resources

Published under the authority of the Department of Energy, Mines and Resources, Government of Yukon http://www.emr.gov.yk.ca.

Printed in Whitehorse, Yukon, 2016.

Publié avec l'autorisation du Ministères de l'Énergie, des Mines et des Ressources du gouvernement du Yukon, http://www.emr.gov.yk.ca.

Imprimé à Whitehorse (Yukon) en 2016.

A copy of this report can be obtained by download from www.geology.gov.yk.ca or by emailing geology@gov.yk.ca.

In referring to this publication, please use the following citation: Klöcking, M., Mills, L., Mortensen, J. and Roots[†], C., 2016. Geology of mid-Cretaceous volcanic rocks at Mount Nansen, central Yukon, and their relationship to the Dawson Range batholith. Yukon Geological Survey, Open File 2016-25, 37 p. plus appendices.

Cover photo: View west from the summit of Mount Nansen.

[†] Deceased, June 2016.

ABSTRACT

The Mount Nansen volcanic complex (MNVC), which is best preserved on Mount Nansen in the southeastern Dawson Range of west-central Yukon, is a 51 km^2 erosional remnant of what was originally a continuous, Early to mid-Cretaceous (115-104 Ma) continental magmatic arc. The MNVC consists of fragmental and massive andesitic flows and minor rhyolite flows and tuff. Two superimposed volcanic successions, with a subtle angular unconformity between them, have been recognized: 1) a lower succession characterized by rhyolitic and andesitic lavas erupted in a proximal vent-environment; and 2) an upper succession dominated by pyroclastic deposits ranging from andesitic block-and-ash breccia to felsic tuff, alternating with andesite flows, interpreted to reflect a more distal setting.

U-Pb zircon dating and lithogeochemical studies of volcanic rocks and spatially associated intrusive rocks, together with field relationships, demonstrate that the volcanism at Mount Nansen was coeval and comagmatic with intrusion of the regional-scale Dawson Range batholith, and formed over a period of ~11 Ma. The volcanic complex in part topographically overlies the main intrusive phases, and is interpreted to have formed an extrusive carapace above the plutonic roots of the arc.

Both the volcanic rocks and nearby granite are cut by northwest, north-northeast and northeast-trending faults and collinear feldspar ± quartz and hornblende-phyric felsic and andesitic dikes.

CONTENTS

Authors left to right: Logan, Marthe, Jim and Charlie.

INTRODUCTION

The Mount Nansen area in west-central Yukon is well known from the more than 30 mineral deposits and occurrences found there. These include epithermal precious metal and polymetallic veins of the Mount Nansen camp (Yukon MINFILE 115I 064 and 065). The region has also been explored for copper-molybdenum porphyry (*e.g.*, the Cyprus porphyry; 115I 066) and potential tin and uranium occurrences. In addition, several of the valleys in the Mount Nansen area have been mined for placer gold since 1899.

Mount Nansen itself is a topographic high point approximately 11 km northwest of the Mount Nansen camp. From its 1827 m (5994 ft) summit, a broad, round-shouldered ridge extends westward with spurs to the north and south. The part of the Mount Nansen area that is above treeline is almost entirely underlain by volcanic rock and dikes of intermediate to felsic composition that are interpreted to be of Early and/or mid-Cretaceous age. It comprises the type area for the Mount Nansen Group (as originally defined by Bostock, 1936). The northern and eastern margins of this area are intruded by granodiorite which represents the southeastern extent of the Dawson Range batholith (Fig.1). Gold-bearing quartz veins were discovered in the Mount Nansen area in 1917, and several underground mining ventures in the 1940s and 1960s led to three open-pit mining operations in the Mount Nansen camp (1968-69, 1976, and 1997-98). Government records indicate that 1234 kg gold and 8304 kg silver were recovered from the various deposits in the Mount Nansen camp (from Yukon MINFILE 115I 064, 065). The Klaza epithermal vein deposit (Yukon MINFILE 115I 067), located 8 km east-northeast of Mount Nansen (Fig. 2), has recently been estimated to contain an inferred resource of 43 000 kg (1.4 Moz) of Au and 840 000 kg (27.0 Moz) of Ag (Ross *et al.*, 2016). Most of the Au-Ag occurrences in the region are contained within the batholith (Allan *et al.*, 2013), whereas mineralization is sparse or absent within the volcanic rocks.

Detailed bedrock mapping of the Mount Nansen highland described in this report provides field constraints on the recognition and distribution of various volcanic facies in the immediate Mount Nansen area and their relationship to local intrusive phases. We have also investigated the age and geochemical character of the various rock units that make up the Mount Nansen Group, together with the Dawson Range batholith and other intrusive phases in the area. The 57 km² area of exposed volcanic rock is one of the largest contiguous remnants of the Mount Nansen Group, which may have once overlain most or all of the Dawson Range. The Mount Nansen area thus represents a vestige of a lost volcanic landscape in western Yukon.

Previous work

Bostock (1936) identified and described the Mount Nansen Group during reconnaissance geological mapping of the Carmacks map area (115I on Fig. 1). As originally defined by Bostock, the Mount Nansen Group included a wide variety of volcanic rocks within the Carmacks map area. Early isotopic ages for these volcanic rocks (*e.g.*, Grond *et al.*, 1984) were mainly obtained by K-Ar whole rock methods. However, many of these ages were subsequently found to reflect resetting in the Late Cretaceous. The term "Mount Nansen Group" was later restricted to latest Early Cretaceous (hereafter "mid-Cretaceous") volcanic rocks by Tempelman-Kluit (1984). Many occurrences of andesite to rhyolite that were initially included in the Mount Nansen Group have been reassigned to other units as more accurate isotopic dating showed them to be either significantly younger or older than mid-Cretaceous (Wheeler, 1961; Tempelman-Kluit, 1984; Breitsprecher and Mortensen, 2004).

Saager and Bianconi (1971) and Sawyer and Dickinson (1976) explored the flanks of Mount Nansen as part of regional exploration programs focused mainly on porphyry style mineralization. Carlson (1987), during systematic regional mapping, provided the first relatively detailed descriptions of the volcanic rocks in the Mount Nansen area. He described andesite flows, subvolcanic intrusions, felsic pyroclastic rocks, and felsic domes in the area, and recognized their intimate relationship with the Dawson Range batholith. Smuk *et al.* (1997) and Smuk (1999) reviewed age information and geochemistry for both the Mount Nansen and

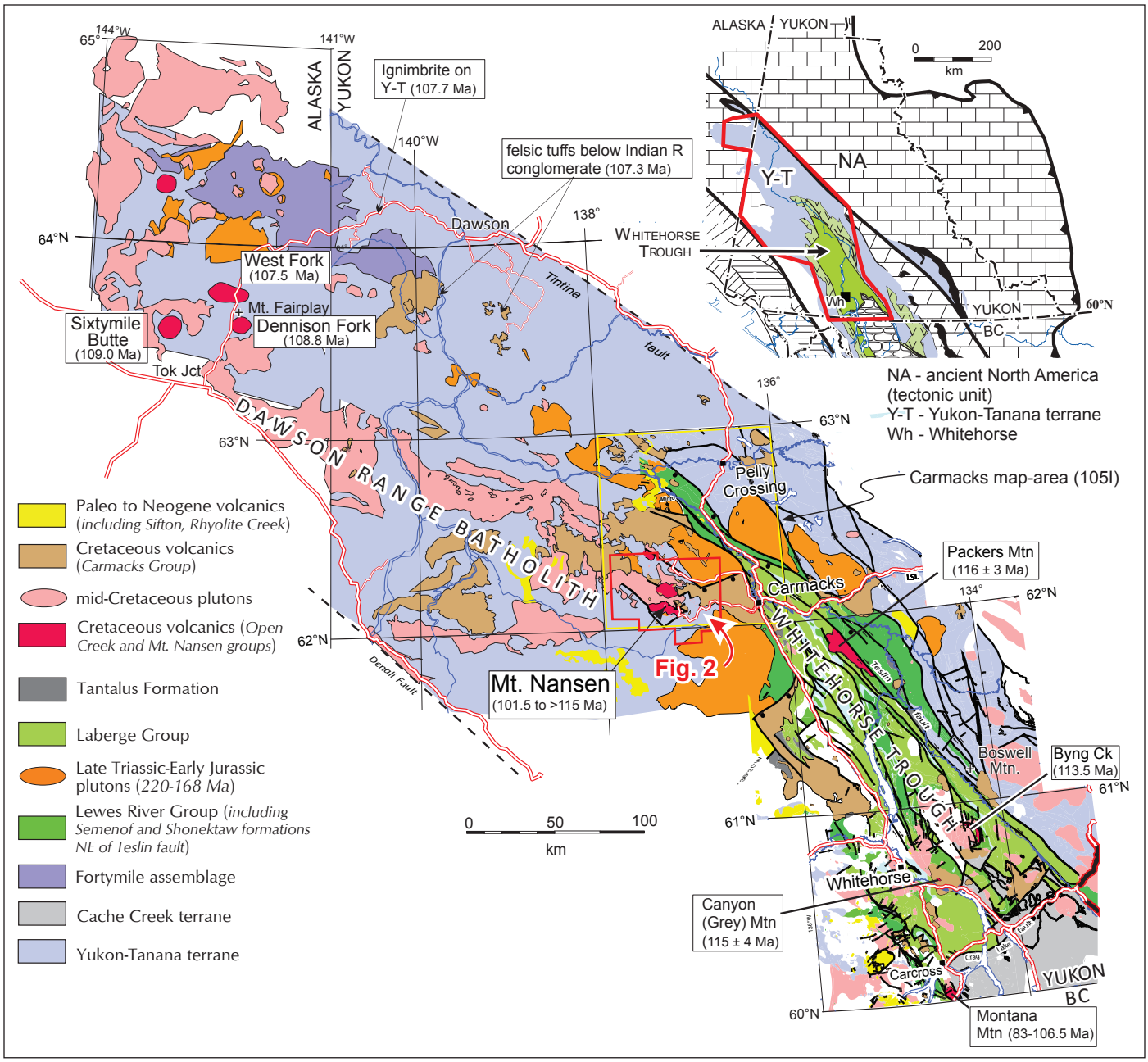

Figure 1. *Regional bedrock distribution showing remnant exposure of two Cretaceous episodes of volcanism (brown, red) and Dawson Range plutonism (pink). Map units selected and modified from regional maps by Bacon et al., 1990; Dusel-Bacon et al., 2006; Colpron, 2011, and Colpron et al., 2016. U-Pb dates of volcanic rocks are recalculated from the sources, with new dates for Mount Nansen in this report.*

the younger Carmacks (73-68 Ma) groups, and postulated that a regional Late Cretaceous hydrothermal event had affected the area and likely reset many of the previously reported K-Ar ages. Hart and Langdon (1998) interpret the Mount Nansen mineral trend to comprise sequentially down-faulted blocks, and suggest that a transition between coeval, relatively deep-seated porphyry Cu-Au mineralization and higher-level epithermal vein systems is preserved in the Mount Nansen area. U-Pb geochronology by Mortensen *et al.* (2003, 2016) confirms that the felsic dikes and stocks that are spatially related to gold mineralization within the Mount Nansen camp were emplaced at ~109-107 Ma. U-Pb dating studies by Mortensen *et al.* (2016) also establish that all of the felsic dikes that are spatially and apparently temporally associated with epithermal Au-Ag-base metal veins in the Klaza camp 8 km east-northeast of Mount Nansen are early Late Cretaceous in age (78-72 Ma).

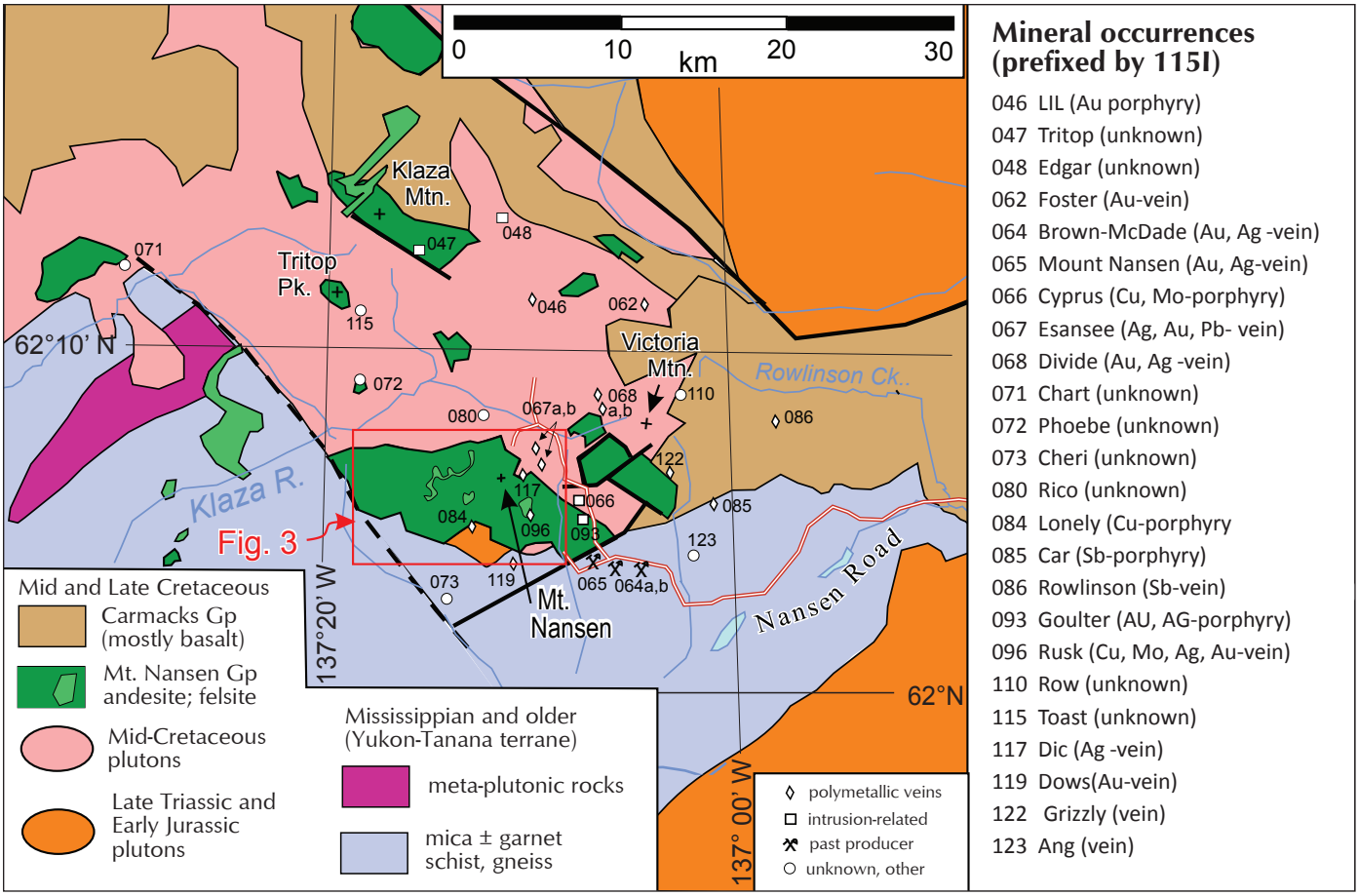

Figure 2. *Simplified bedrock units of west-central Yukon, showing distribution of two Cretaceous volcanic groups (modified from Colpron, 2011) and mineral occurrences (from Yukon MINFILE).*

The Mount Nansen area and Nisling River drainage to south and west have been the focus of on-going regional bedrock mapping by Ryan *et al.* (2016).

Present work

The area was selected for detailed study because it affords relatively abundant exposure and, despite being the type area for the "Mount Nansen Group", no detailed mapping of the volcanic units (with the exception of reconnaissance scale mapping by Carlson, 1987) has been done, nor has any petrographic, lithogeochemical or geochronological study of the volcanic units been completed. Accordingly, 25 days of mapping traverses were conducted from lightweight camps, which were moved periodically by helicopter. The work encompassed almost every ridge-top bedrock exposure. Outstanding features were photographed and samples selected for petrography. Bedrock maps were prepared at 1:15 000 scale which, together with a report summarizing rock examination, satisfied course requirements at the University of Cambridge for the first two authors (Klöcking, 2012; Mills, 2012).

Nine samples were age dated using U-Pb zircon methods, and whole-rock geochemical analyses were completed on 16 samples that are representative of the main extrusive and intrusive rock units in the study area.

The results of these cartographic, petrographic, geochemical and geochronological studies are integrated with previously published work on the volcanic rocks in the Mount Nansen area and with potential regional correlatives. This report provides an interpretation of successive stages of magmatism that were responsible for development of the Mount Nansen Group in its type area.

In this report we refer to the volcanic and associated dike assemblage present on Mount Nansen itself as the Mount Nansen volcanic complex (MNVC), rather than Group, in order to comply with formal nomenclature as defined by the North American stratigraphic code; a 'complex' is defined as an unranked lithodemic unit, including two or more classes of rocks that are intermixed and inseparable at a detailed scale of mapping (NACSN, 2005; Owen, 1987). Our mapping of the MNVC (described in this report) identifies several distinct rock units, but was not sufficiently detailed to permit confidently assigning relative stratigraphic positions to these units. In view of this lack of stratigraphic detail the volcanic sequence cannot be assigned Group status. The MNVC in the Mount Nansen area, as described herein, includes massive aphyric or feldspar-phyric andesite to dacite flows, breccia and tuff, massive heterolithic, quartz and feldspar-phyric felsic lapilli tuff, flow banded quartz-phyric rhyolite and quartz-feldspar porphyry plugs, dikes, sills and breccia.

REGIONAL TECTONIC SETTING

The Mount Nansen Group (*sensu lato*) consists dominantly of remnants of volcanic edifices depositionally overlying basement rock units that comprise the Yukon-Tanana and Stikine terranes and the Whitehorse trough (Figs. 1 and 2). The present distribution of the Mount Nansen Group roughly coincides with the more extensive late Early Cretaceous Whitehorse plutonic suite (Wheeler and McFeely, 1991; Mortensen *et al.*, 2000; Gordey and Makepeace, 2003; Hart *et al.*, 2004).

Yukon-Tanana terrane in the Mount Nansen area includes Devonian-Mississippian arc and back-arc assemblages built on older continent-derived sedimentary rocks (Mortensen, 1992; Colpron *et al.*, 2006; Nelson *et al.*, 2006), which in western Yukon were subjected to Permian intrusion and metamorphism (Gordey *et al.*, 2006; Berman *et al.*, 2006; Beranek and Mortensen, 2011; Ryan *et al.*, 2013). Stikine terrane (Stikinia) developed along the western edge of the North American plate in the Late Triassic to Early Jurassic (Tempelman-Kluit, 1979; Mihalynuk *et al.*, 1994). It is an 'overlap assemblage' atop a basement that comprises Upper Devonian to Permian volcanic and co-magmatic plutonic rocks of the Paleozoic Stikine Assemblage in northern British Columbia and southern Yukon, and the Yukon-Tanana terrane in western Yukon (Monger *et al.*, 1991; Hart, 1997). This overlap assemblage comprises Late Triassic to Middle Jurassic volcanic and sedimentary strata, as well as extensive Late Triassic to Early Jurassic granitic plutons, including the Aishihik and Long Lake plutonic suites (Johnston *et al.*, 1996a) and the Big Creek syenite of Carlson (1987), all of which intrude the Yukon-Tanana terrane (Currie and Parrish, 1997; Colpron *et al.*, 2003; Colpron and Ryan, 2010).

East-dipping (present coordinates) subduction along the margin of northwestern Laurentia beginning in the Late Triassic (Nelson and Colpron, 2007) produced a series of continental volcanic arcs that developed progressively westward across the Stikine and Yukon-Tanana terranes.

The Whitehorse trough is an Early to Middle Jurassic successor basin that overlies the northern Stikine terrane. More than 7000 m of clastic strata were deposited (Wheeler, 1961; Hart, 1997; Colpron, 2011). During the Late Jurassic and Cretaceous the trough was tectonically shortened, uplifted and folded, and dismembered by dextral transpressive faults (Colpron *et al.*, 2006).

The mid-Cretaceous Dawson Range batholith (Tempelman-Kluit, 1984; Payne *et al.*, 1987) has been interpreted by many as the plutonic roots of a volcanic arc (*e.g.*, Mortensen *et al.*, 2000; Hart *et al.*, 2004). Others, however, suggest that some phases of the Dawson Range batholith may be crustally derived (*e.g.*, Selby *et al.*, 1999; Zagorevski *et al.*, 2014). Plutons were emplaced into the Stikine and Yukon-Tanana terranes and now underlie much of the Dawson Range itself (Fig. 1). The Dawson Range batholith may have a sheet-like geometry (Johnston and Shives, 1995; Hart and Langdon, 1998). As described in this report, the andesitic to felsic centres of the Mount Nansen Group are equivalent in age to the underlying plutonic rocks. Orthogonal fault sets that crosscut the batholith and Mount Nansen Group volcanic rocks provide strong structural control on mineralization throughout the region (Sanchez *et al.*, 2013).

During the Late Cretaceous, flood basalt was extruded from vents in the Carmacks area (Bostock, 1936; Tempelman-Kluit, 1984, 2009; Johnston *et al.*, 1996b; Smuk *et al.*, 1997; Smuk, 1999). These lava flows, which comprise most of the Carmacks Group, unconformably overlie older basement units, as well as the Mount Nansen Group. Rhyolitic volcanic rocks and clastic fill assigned to the Carmacks Group are locally preserved. Subsequently (although some occurrences may be earlier; isotopic dating is incomplete), clusters of predominantly felsic calderas of Paleocene and Eocene age developed within the rising Coast Plutonic Complex (Sifton-Skukum-Sloko suite: Lambert, 1974; McDonald, 1990, Sifton Range: Miskovic and Francis, 2004, Rhyolite Creek volcano-plutonic complex: Israel and Borch, 2015) as well as the Yukon-Tanana upland (Fig. 1). Most recent are basalt flows and cinder cones of the Miocene through Neogene Northern Cordilleran volcanic province that have been interpreted as the product of a deep seated source (possibly slab window; Hart and Villeneuve, 1999; Edwards and Russell, 2000).

REGIONAL DISTRIBUTION OF THE MOUNT NANSEN GROUP

In the southeast Dawson Range (Fig. 1) exposures of Mount Nansen Group volcanic rocks occur at relatively high elevation, where they non-conformably overlie Yukon-Tanana metamorphic basement as well as the Triassic-Jurassic and mid-Cretaceous intrusive rocks. The MNVC on Mount Nansen itself is the largest preserved mid-Cretaceous volcanic paleo-landscape in Yukon. Erosion of the MNVC has led to the development of volcanic 'islands' surrounded by a 'sea' of granite. It is likely that some smaller 'islands' and dike swarms represent feeders or volcanic necks.

Widely separated occurrences of volcanic rocks roughly age-equivalent to the MNVC occur outside the Mount Nansen area in southern and southwestern Yukon and eastern-most Alaska. The character of several of these occurrences is described below to provide regional context for the detailed study of the MNVC.

On the flanks of Victoria Mountain, 12 km northeast of Mount Nansen (Fig. 2), a roughly 20 km^2 area of coarse-grained andesite flows and agglomerate assigned to the Mount Nansen Group is intruded by a gabbroic stock and northeast trending hornblende-feldspar, and less commonly felsic, dikes (Carlson, 1987). Andesitic flows and breccia presently assigned to the Mount Nansen Group also cap Tritop Peak and Klaza Mountain, 17 km and 22 km northwest of Mount Nansen respectively. Exposures farther north and west are predominantly felsic flows and breccia (Tempelman-Kluit, 1984). K-Ar analyses of a mauve-grey felsic rock from Klaza Mountain resulted in an age of 109 ± 3 Ma (K-Ar; Stevens *et al.*, 1982). Crosscutting the granite are numerous northeast-trending felsic dikes and sills, including a 100 m thick rhyolite sill within Yukon-Tanana schist 17 km west of Mount Nansen (Tempelman-Kluit, 1984; 2009). These intrusions constrain the broad regional stress field present during the latter stages of Mount Nansen Group volcanism.

Correlatives of the Mount Nansen Group farther to the southeast overlap Whitehorse trough sedimentary rocks (Jurassic Laberge Group), where they are commonly preserved by syn or post-volcanic normal faulting. On Packers Mountain, 48 km southeast of Carmacks (Fig. 1), a 35-km-long exposure of rusty weathering, fine-grained dacite and rhyolite interpreted to be MNVC (Tempelman-Kluit, 1984) locally unconformably overlies the upper Triassic Lewis River group. Flow banded rhyolite sampled from this locality returned a K-Ar age of 116 ± 3 Ma (K-Ar; Stevens *et al.*, 1982; Colpron *et al.*, 2007). A smaller occurrence about 70 km farther to the south-southeast, just west of Boswell Mountain, consists of dark green massive andesite and breccia (Tempelman-Kluit, 2009).

The Byng Creek volcanic complex, a subcircular occurrence of volcanic rocks 40 km east of Whitehorse (Fig. 1), consists of subaerial intermediate to felsic flows and pyroclastic rocks that non-conformably overlie granite and folded Whitehorse trough sedimentary rocks (Hart, 1997). Locally present beneath the volcanic rocks is a basal conglomerate composed of well-rounded pebble to cobble size granitic and volcanic clasts. In other places older granodiorite has been shattered and milled, presumably by explosive emplacement of the volcanic rocks. The volcanic rocks are intruded by dacite porphyry sills and dikes. Felsic tuff in the Byng Creek complex has a U-Pb zircon age of 113.5 Ma (Hart, 1997), which is essentially coeval with the

nearby Byng Creek granitic pluton. The variety of brecciated rocks and an arcuate fault along the eastern perimeter of the Byng Creek volcanic complex suggest that this is a deeply eroded remnant of a nested caldera complex that is about 15 km in diameter (Hart, 1997). The abundant felsic dikes in the area have not been dated.

On the west side of Canyon (Grey) Mountain, 4 km southeast of Whitehorse, a volcaniclastic deposit up to 85 m thick unconformably overlies Lewes River Group limestone (Dorsey, 2013). Detrital zircon recovered from the unit includes grains as young as 115±4 Ma (M. Colpron, pers. comm., 2009). The conglomerate, which includes angular cobbles of plagioclase-phyric andesite, must be younger than this date; it may be an erosional outlier of the Mount Nansen Group, although there is no evidence for its source.

Montana Mountain, 10 km south of Carcross (Fig. 1) is a subcircular 110 km² area dominated by thickly layered massive and fragmental andesite, with stratigraphically higher rhyodacite pyroclastic flows (Roots, 1981, 1982). The outer contact of the volcanic rocks to the south and west lies in deep valleys, which suggests that the volcanic rocks were preserved by subsidence on ring-faults. The northern margin of the volcanic assemblage is intruded by granite of the Whitehorse plutonic suite that is dated at 106.5 Ma (U-Pb zircon; Hart, 1995), hence the overlying flows must be older. A west-trending vertical fault bisects the volcanic complex, juxtaposing the andesitic flows of the northern half of the complex against stratigraphically higher units of the southern half. An andesitic pyroclastic breccia and a flow banded rhyolite from the southern half of the complex have been dated at 94 and 83 Ma respectively (U-Pb zircon; Hart and Radloff, 1990), implying that volcanism in the Montana Mountain area occurred over a span of 20 million years. Only the older part of the volcanic sequence in this area is considered to be stratigraphically correlative with the Mount Nansen Group. Flat-lying tuffs and andesitic breccia comprise minor occurrences east of Montana Mountain and 26 km west of Carcross (Hart and Radloff, 1990).

Widespread exposures of mafic and felsic rocks near Mount Fairplay in eastern Alaska (Fig. 1) include some recognized caldera structures (Bacon *et al.*, 1990) with U-Pb zircon ages in the range of 110-107 Ma (Mortensen and Dusel-Bacon, 2014). Distal felsic ash horizons and a single occurrence of welded ignimbrite that yield similar U-Pb zircon ages have been recognized at several localities in the southwestern Dawson and northern Stewart River map areas in western Yukon (Fig. 1; Mortensen and Dusel-Bacon, 2014); these more distal occurrences are interpreted to be related to either the eastern Alaskan calderas or to other, not yet identified, caldera eruptions in western Yukon. These calderas are within the age range of the Mount Nansen Group and are considered to be the northwestern extension of this volcanic belt.

Regionally, the Mount Nansen Group encompasses eruptive products from a number of subaerial andesite to rhyolite eruptive centres. Collectively, these are interpreted to constitute a continental volcanic arc that developed obliquely to the regional structural grain defined by the Whitehorse trough and mostly overlapping the Yukon-Tanana terrane. The arc is interpreted to be a product of east-dipping subduction.

Volatile rich magma led to explosive eruptions (abundant breccia) and development of several calderas. Several centres of the Mount Nansen Group and related volcanic rock were intruded by coeval granitic plutons. In southern Yukon the Mount Nansen Group correlatives display successions hundreds of metres thick, suggesting depressions or subsidence; in contrast those in west-central Yukon appear to be erosional remnants at high elevation. Some of the latter may have been part of a more extensive volcanic field. Many possible vent areas may have been eroded to the level of subvolcanic felsic dike swarms and plugs. No age progression in these volcanic centres has been recognized. Neither large ash-flow deposits nor intra-caldera sediment have been identified in Yukon thus far, although such deposits are present in the vicinity of the coeval calderas in eastern Alaska.

GEOLOGY AND GEOCHRONOLOGY OF THE MOUNT NANSEN AREA

The general geology of the Mount Nansen area is shown in Figure 3, and localities mentioned in the text are shown on this figure and summarized in Table 1. In the following sections we describe the outcrop characteristics of the various rock units in the Mount Nansen area, together with structural and textural features that bear on the nature of each unit. We also discuss U-Pb zircon age determinations for nine rock samples (summarized in Table 2), and utilize these data to constrain the temporal evolution of the MNVC.

U-Pb zircon dating results described in this report were obtained using laser ablation (LA-)ICP-MS methods at the Pacific Centre for Isotopic and Geochemical Research (PCIGR) at the University of British Columbia. Analytical methodology follows that described in Tafti *et al.* (2009) and Beranek and Mortensen (2011). The $^{206}Pb/^{238}U$ age is the most precisely determined age for Phanerozoic zircons and is interpreted as the best estimate for the crystallization age of the samples. Assigned ages are based on a weighted average of overlapping concordant $^{206}Pb/^{238}U$ ages of individual analyses for each sample. Errors are quoted at the 2σ level. Analytical data are given in Appendix 1 and are presented in conventional U-Pb concordia diagrams and weighted average $^{206}Pb/^{238}U$ age summary plots in Figure 4 and two later figures.

Pre-Cretaceous units

Highly strained metamorphic and plutonic rocks non-conformably underlie the MNVC volcanic rocks to the south and west of Mount Nansen. These rocks were previously referred to as the Wolverine metamorphic complex (Johnston and Hachey, 1993; Johnston, 1995; Selby *et al.*, 1999); however, they are now assigned to two assemblages of Yukon-Tanana terrane (Colpron *et al.*, 2006). Outcrops of quartzite, and schist containing hornblende-rich pods and garnet porphyroblasts, lithologically resemble and are tentatively correlated with the pre-Devonian Snowcap assemblage (Colpron and Ryan, 2010). Quartz-muscovite schist with discrete biotite rich layers revealing multiple deformation phases (Fig. 5) is correlated with the Devono-Mississippian Finlayson assemblage. Both assemblages extend south of Mount Nansen (Israel and Westberg, 2012), where Finlayson assemblage rock units are separated from Snowcap to the west by a northwest trending fault (Colpron, 2011).

Orange-brown weathering, weakly foliated granodiorite to quartz monzonite (Fig. 6) is exposed at the tips of two ridge spurs 2.5 km south of Mount Nansen. This intrusive phase had previously been considered to be part of the Dawson Range batholith by Carlson (1987). The contact of the granite is parallel to foliation of the schist and amphibolite, suggesting that the granite may be a northwest dipping sheet in this area.

Zircons from a sample of this granodiorite are clear, colorless, stubby to elongate prisms with faint igneous growth zoning. Clear bubble and rod-shaped inclusions are common in many grains, but no inherited zircon cores have been observed. Twenty zircon grains from sample LM370 all yielded overlapping concordant analyses with a weighted average $^{206}Pb/^{238}U$ age of 211.1 ± 0.9 Ma (Figs. 4a,b; Appendix 1), which is interpreted to be the emplacement age of the intrusion.

This Late Triassic age is consistent with the known age range of the Stikine plutonic suite (Colpron, 2011; Colpron *et al.*, 2016). A similar U-Pb zircon age (211.4 ± 3.3 Ma) was obtained for zircons from a sample of biotite-hornblende granodiorite which hosts the Dickson deposit in the Mount Nansen camp (Fig. 2, about 200 m north of mineral occurrence 64a; Mortensen *et al.*, 2003, recalculated in Colpron, 2011). Titanite crystals from this sample yielded a U-Pb age of 191.5 ± 2.9 Ma (Mortensen *et al.*, 2003). These intrusions into Yukon-Tanana terrane are typically deformed, in contrast to the Early to mid-Jurassic plutonic suites (Long Lake, Aishihik) in the same region.

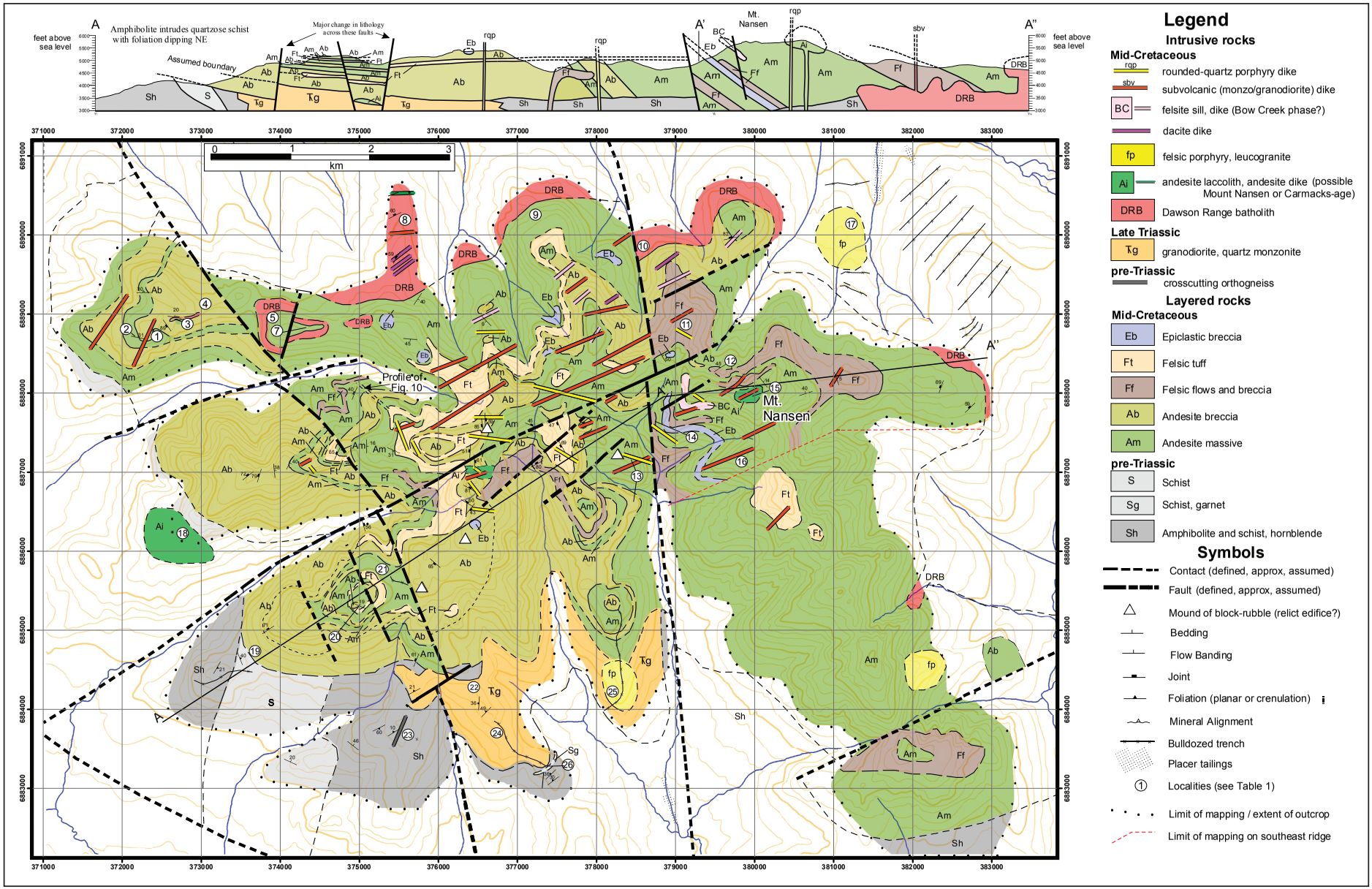

Figure 3. *Bedrock geology of Mount Nansen volcanic complex (simplified from unpublished 1:15 000 maps). Rock units of the southeast ridge are modified from Carlson (1987); our detailed mapping ends at the red dashed boundary. Circled numbers indicate localities of interest described in Table 1 and cited in the text.*

Table 1. *Localities of interest (circled on Figure 3 - map).*

#		UTM (NAD 1927 datum)
1	Vertical bands of variably glassy material in andesite indicate streaming alteration and possibly vertical movement of magma.	372352 6888809
2	Swirled, ragged fragments in breccia consistent with churning in a volcanic vent setting.	372194 6888710
3	Granophyric sill with joints possibly contraction columns.	372656 6888967
4	Isolated pillar reveals sub rounded granophyric clasts, 60 cm in diameter, in andesite breccia.	373080 6889173
5	Apophyses of fine-grained K-spar rich granodiorite intrude andesite.	373889 6888950
6	2 m wide dike composed of 3 mm hornblende needles in a felsic groundmass.	375478 6890276
7	Observation of dextral shear supports adjacent SE trending fault.	374251 6888850
8	Breccia with subrounded heterolithic cobbles in mud-sand cement interpreted as epiclastic.	375629 6888676
9	Irregular intrusive contact implied by granitic felsenmeer up-slope of exposed volcanic-plutonic contact.	377308 6893950
10	Regional aeromagnetic response and distribution of granite outcrop support N-S fault with dextral displacement.	378500 6889900
11	Spherulitic devitirification in felsenmeer of rhyolite lava.	374101 6888867
12	Snowflake devitrification in felsenmeer of rhyolite lava.	379800 6888231
13	Jasper commonly occurs in this area, particularly as the matrix for breccia.	378153 6886667
14	Planar spherulitic devitrification of rhyolite, suggesting viscous lava flow.	378894 6887460
15	The summit exposes abundant relatively fresh hornblende phenocrysts; possibly andesite laccolith.	380103 6888147
16	Good outcrop up to 2 m high of pink weathering monzogranite dike.	379556 6887145
17	Circular plug of felsic porphyry reinterpreted as leucogranite is transcribed from Carlson, 1987.	381000 6890000
18	Homogenous andesite porphyry, similar to the main summit of Mt Nansen. Isolated exposure is well defined by aeromagnetic response.	376909 6885199
19	Volcanic contact with schist clearly expressed by aeromagnetic response; could be fault or unconformity.	373122 6884387
20	Massive andesite 15 m high possibly columnar jointed; implies basal layer dips 10° NE.	374914 6885324
21	Massive andesite with high magnetic susceptibility (up to $38x10^{-6}$ cm^3mol^{-1}).	375087 6885634
22	Foliation in the Late Triassic granite is parallel to the foliation in the amphibolite.	376619 6884010
23	4 m thick sheet of orthogneiss; possibly Simpson Range Orthogneiss.	375719 6884259
24	Leucogranitic dikes intrude the Late Triassic granite in this area.	377268 6883315
25	Rusty, leached, medium grained leucogranite hosts the Lonely Cu-Mo occurrence.	378259 6885237
26	Almandine porphyroblasts up to 8 mm in schist band 20 m wide.	377470 6883136

Table 2. *Summary of U-Pb zircon dating results.*

Sample	Map-unit	Lithology	Age ± 2σ error
LM370	Tg	weakly foliated hornblende-(biotite)-phyric tonalite	211.1 ± 0.9 Ma
MK060A3	DRB	granitic clast in andesitic volcanic matrix	105.2 ± 0.5 Ma
LM401C1	Ab	plagioclase-phyric andesitic clasts within pyroclastic breccia	112.2 ± 1.8 Ma
LM401C2	Ab	plagioclase-phyric andesitic clasts within pyroclastic breccia	115.2 ± 1.7 Ma
MK371	Ff	feldspar-phyric grey felsic flow	107.4 ± 0.7 Ma
LM247	DRB	hornblende-phyric unfoliated granodiorite; part of Dawson Range Batholith	107.1 ± 0.8 Ma
LM223A2	Ai	quartz-plagioclase-phyric andesite dike	105.9 ± 0.4 Ma
LM484	BC	pink crystalline kspar-hornblende-phyric felsic intrusion	104.7 ± 0.8 Ma
LM130A2	sbv	hypabyssal hornblende-phyric granodiorite dike	103.8 ± 0.5 Ma

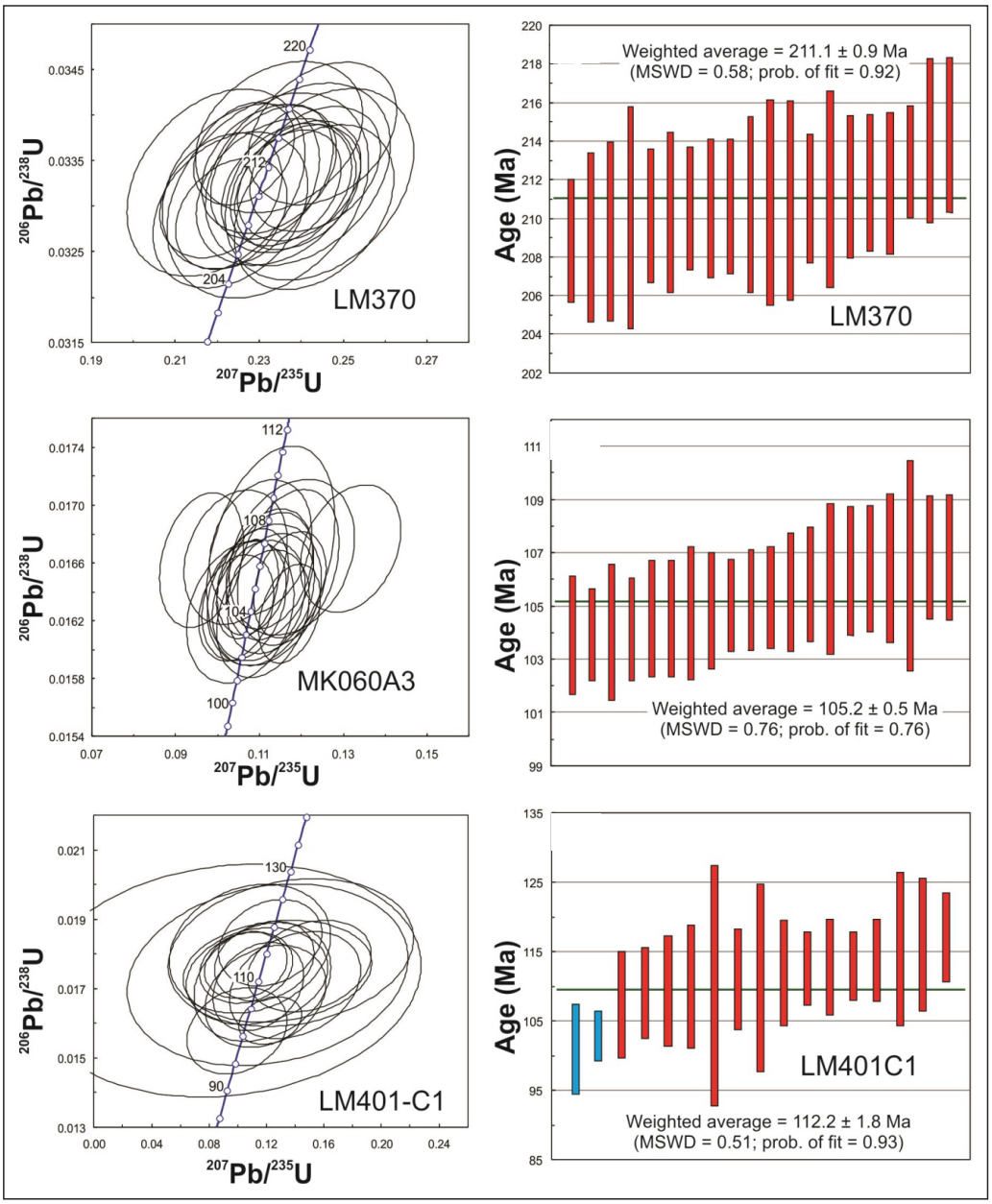

Figure 4. *U-Pb concordia diagrams and weighted average $^{206}Pb/^{238}U$ age summary plots for: a, b) LM370 (foliated granodiorite); c, d) MK060A3 (granitic clast in andesite breccia); and e, f) LM401C1 (andesite clast in breccia). Analytical results are in Appendix 1; those shown as blue bars are excluded from the weighted average age calculation. All errors are shown at the 2σ level.*

Figure 5. *Tight isoclinal folds in map-unit 'S', likely a mafic metavolcanic rock of the Finlayson assemblage, Yukon-Tanana terrane. UTM zone 8V, 374748E 6883716N.*

Figure 6. *Late Triassic foliated granodiorite to quartz monzonite (map-unit 'Tg') contains hornblende, biotite and epidote. Scale graduations are mm. 378060E 6884040N.*

Extrusive rocks (Mount Nansen volcanic complex - MNVC)

Volcanic bedrock at Mount Nansen forms isolated knobs and small peaks that are separated by talus slopes and wide valleys. Fresh surfaces of most of the exposed volcanic units are dark-coloured, and commonly breccia clasts are faintly discernible on weathered surfaces of fragmental units. Contacts between map units are seldom obvious from a distance. Rhyolite to dacite (here collectively referred to as felsic) units were easily distinguished in hand sample but only the rounded quartz porphyry dikes and some tuff horizons could be identified from a distance (pale weathering rubble). Detailed study of weathered rock surfaces, structural or lithological contacts inferred from topography, together with geochronology of selected samples, were the principal mapping tools for the MNVC. The nature of other dikes were determined from outcrop examination and crosscutting relationships, corroborated by U-Pb dating.

Most of the volcanic rocks in the MNVC are undeformed and, where geopetal fabrics or textures are evident, stratigraphy is upright. Topographic relief, from the lowest volcanic outcrop to the summit of Mount Nansen, is 450 m, and this is a minimum thickness for the preserved volcanic succession. The un-roofing of medium and coarse-grained granodiorite north of the volcanic rocks that non-conformably underlies the eruptive units indicates that a significant amount of overlying rock must have been removed since emplacement of the plutons.

No distinctive time-marker horizons, such as ash layers, were found among the massive and fragmental flow units. The map units are therefore defined on the basis of lithology: andesitic lava flows and breccia, felsic flows and breccia, and epiclastic deposits (Fig. 3). Some of these units are tabular, whereas others interdigitate and/or occur more than once in the volcanic succession. Volcanic outcrops at lower elevations reveal locally variable primary attitudes, whereas those along ridge crests are typically gently dipping. From these clues of primary structure it is possible to recognize separate volcanic successions with distinct facies interpretations (*see* discussion which follows unit descriptions).

Four subcircular-shaped piles situated on ridge tops consist of large blocks of porphyritic andesite (Fig. 7; rubble mound symbol on Fig. 3). The largest is about 20 m high and 90 m in diameter; the smallest recognized is 5 m high and 20 m diameter. Outcrop is absent in these areas, but the rubble blocks contrast with the underlying massive andesite. The subcircular plan of each suggests a conduit or vent area, although *in situ* evidence is lacking.

Another exposure of a possible vent lies about 7 km west-northwest of Mount Nansen (locality 2, Fig. 3). An andesitic outcrop less than 100 m across displays steep compositional layering (Fig. 8), surrounded by a subcircular zone of ash-sized breccia containing shattered angular andesitic clasts and tuff with intricate flow structures.

Andesite flows

Dark green, light grey and ochre weathering, massive andesite with variable feldspar phenocryst content and a dark grey-green groundmass comprise large expanses of frost-heaved rubble on ridges (map unit Am, Fig. 3). Blocky outcrops and low walls are formed by spalling along steep joint sets. On some ridges a prominent joint set normal to presumed bedding may reflect cooling fractures (columnar jointing) of flat-lying flows or sills (Fig. 9). Layering on one northwest-trending spur consists of flows 10 to 30 m thick, separated by breccia (map unit Ab) and thin felsic tuff horizons (Fig. 10). Clast-supported monolithologic andesite breccia (Fig. 11) is interpreted to represent rubbly flow-tops formed during or shortly after eruption.

Figure 7. *Rubble mounds on ridge crest and sub-horizontal exposure of flows and breccia deposits. View southeast from 0375234E 6888879N; MK 080.*

Figure 8. *Steeply dipping bands in porphyritic andesite; interpreted as a pipe to a vent (surrounded by breccia), near locality 2; 372352E 6888709N.*

Figure 9. *Massive andesite displaying steep polygonal jointing suggestive of cooling fractures. Note gently dipping color bands near base. 374914E 6885324N; LM 168.*

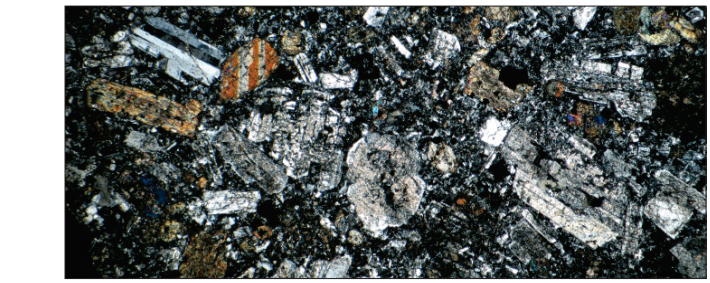

MK 030: basaltic andesite flow with groundmass showing more crystallization than other sampled flows. Phenocrysts comprise at least 60%: twinned plagioclase up to 5 mm long and clinopyroxene. Much less altered than underlying flows.

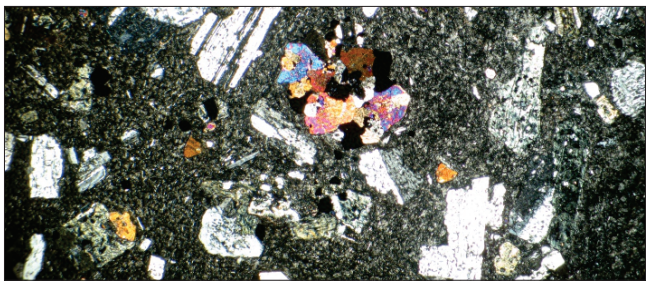

LM 052: andesite flow with fine-grained groundmass and 35% plagioclase phenocrysts up to 4 mm long, and more clinopyroxene than other sampled flows.

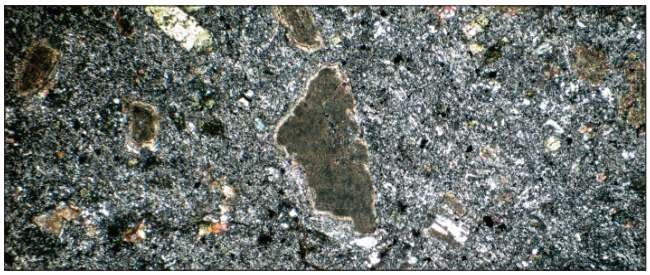

LM 056: andesite flow with plagioclase microlite groundmass and 15% plagioclase phenocrysts. Alteration is greater than LM 057, showing pervasive sericite and rims of clay minerals.

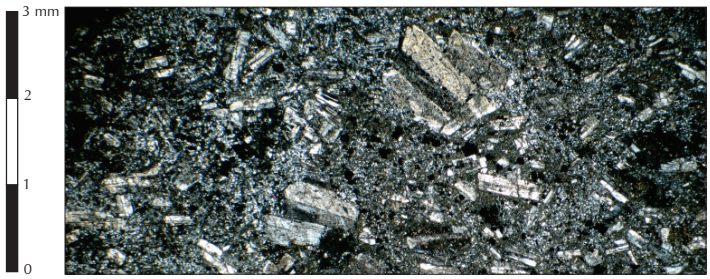

LM 057: andesite flow with fine-grained groundmass and bimodal size distribution of phenocrysts.

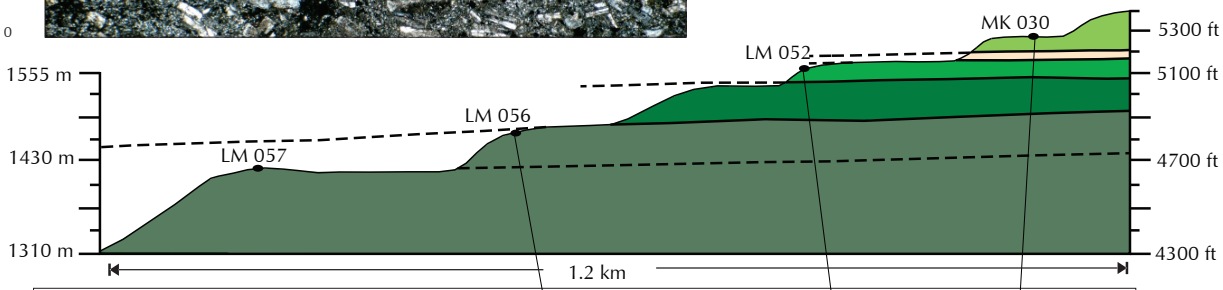

Figure 10. *Northeastward view of a succession of andesite flows on a northwest spur (see Fig. 3). Textures revealed in thin sections from representative samples along the spur. Note the variation in degree of crystallinity and alteration. Most contain plagioclase with incipient twinning and smaller clinopyroxene phenocrysts within a groundmass of plagioclase microlites. Scale is same for all photomicrographs.*

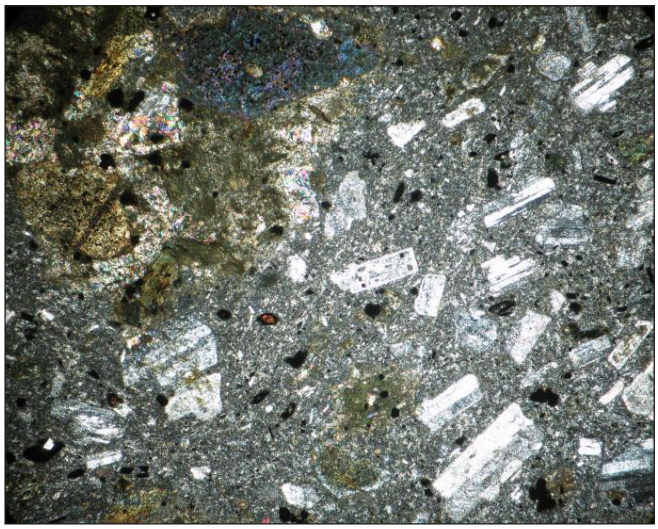

Figure 11. *Mineral alignment in an andesite flow on Mt. Nansen. Width of view: 7.1 mm. 380126E 6887627N; LM 255.*

Despite relatively good exposure, contacts were rarely recognized within the andesite unit and it is difficult to determine whether some of the massive exposures represent flows and/or tabular intrusive bodies (laccoliths). The interpretation of at least some of the massive andesite as flows is supported by the observation of quartz filled vesicles (which would be more common in extrusive rocks), and local gradation from massive andesite upwards into monolithologic breccia (possibly lava-flow margin).

The paucity of massive andesite among extensive breccia in outcrop increases our confidence that andesitic intrusions (map unit Ai**)** are relatively uncommon.

The andesite is mostly porphyritic, containing 15 to 60% tabular phenocrysts of hornblende and plagioclase (up to 6 mm long, mostly of white to cream-colored feldspar; An_{40-70}) in a fine-grained crystalline and glassy matrix. Phenocrysts locally have rounded edges and corners that indicate partial resorption. The massive andesite locally contains minor biotite or clinopyroxene, rare olivine, and sphene or magnetite as accessory minerals. In some outcrops phenocrysts are aligned, defining a vague fabric that may be parallel to primary layering, with dips ranging from sub-horizontal to about 40° (Fig. 12).

Flow banding is locally visible in the andesite as parallel, planar banding of colour or texture (Fig. 13). The flow banding may have resulted from semi-viscous movement within a lava flow or in a conduit, such as a dike or below a volcanic vent. The preferred orientation of tabular phenocrysts, which is seen locally, is thought to provide better evidence than any observed planar features to indicate orientation of the original layering in lava flows.

Andesite breccia

Fragmental volcanic rocks are the most extensive lithology at Mount Nansen. Unfortunately, textures are commonly obscured by lichen and the dark groundmass, except where weathering reveals the presence of clasts by color or differential relief; the proportion of breccia present within the andesite unit is therefore unclear. Clast-size and texture vary within the breccia, from granule to large blocks (0.5-200 cm), and from

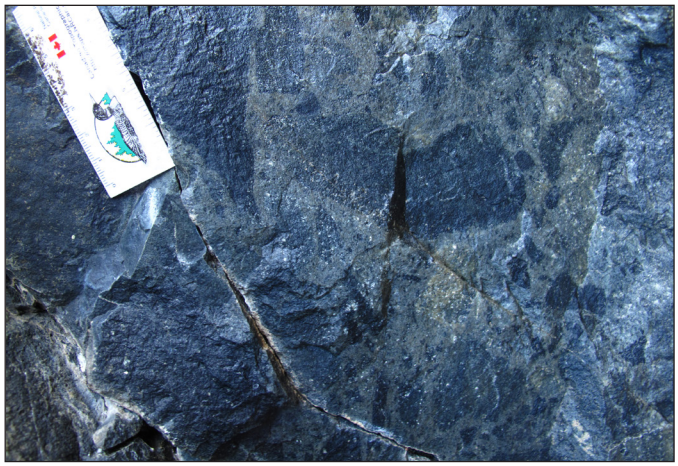

Figure 12. *Monolithologic breccia showing subrounded andesite clasts in igneous matrix, interpreted to have formed on lava flows or collapse of andesitic vent. Scale bar is 15 cm long. 378138E 6889355N; LM 479.*

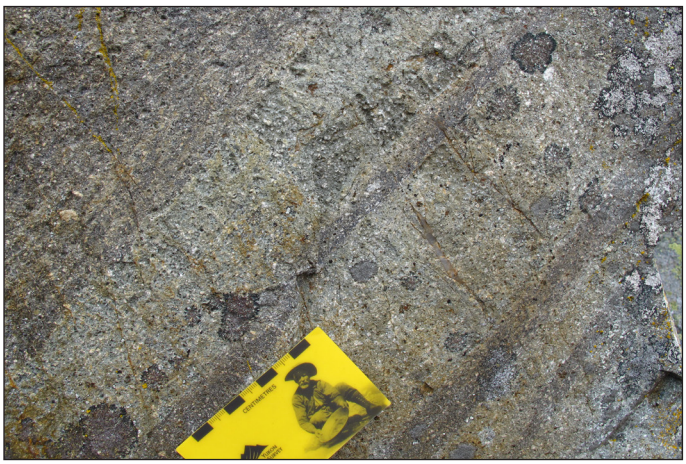

Figure 13. *Steep flow banding in andesite (unit* Ai*) near Mt. Nansen, scale bar is 9 cm long. 375275E 6889147N; LM 224.*

rounded to angular (Fig. 14). Almost all of the fragments in the breccia are cognate volcanic material. Typically andesite clasts have rounded edges and appear to be supported in a fine-grained or grainy groundmass of igneous derivation. Although in some good exposures crude size stratification is evident, clast sorting is typically poor.

In the northwest part of the complex (locality 4 on Fig. 3) subrounded granitic clasts up to 50 cm in diameter occur within andesitic volcanic matrix (Fig. 15). The fine-crystalline matrix of this breccia contains phenocrysts of plagioclase and hornblende which are mostly resorbed (Fig. 16), a texture demonstrating alteration, and possibly through incorporation in a hot andesitic volcanic vent. The matrix appears to be primary; it is interpreted to have been molten when the clasts were incorporated. No vesicles or porous material were noted in these breccia units.

The granite clasts have a fine-grained groundmass, which differs from the textures in typical Dawson Range batholith exposures in the area. Zircons separated from one granitic clast (sample MK060A3) were dated using U-Pb methods (Fig. 4c,d; Appendix 1). Twenty individual grains give overlapping U-Pb results with a weighted average $^{206}Pb/^{238}U$ age of 105.2±0.5 Ma, which is interpreted to provide the crystallization age of the clast. The andesite flow that entrained the clast must be younger than this. It is possible that the andesite lava entrained pieces of subvolcanic granitic intrusion during its extrusion from the volcanic edifice. Alternatively the clasts may represent weathered and subsequently eroded granitic exposures of the upper part of the Dawson Range batholith that were engulfed by a later lava flow.

The majority of clasts in the breccia are andesitic and compositionally resemble the matrix and adjacent massive lithology; however, clasts of other compositions, including

Figure 14. *Block-and-ash breccia, showing a mixture of angular and rounded clasts, some with diffuse margins indicating partial disaggregation resulting from heat and movement. Note also subtle size stratification. Scale graduations are mm. 376856E 6888125N; MK 101.*

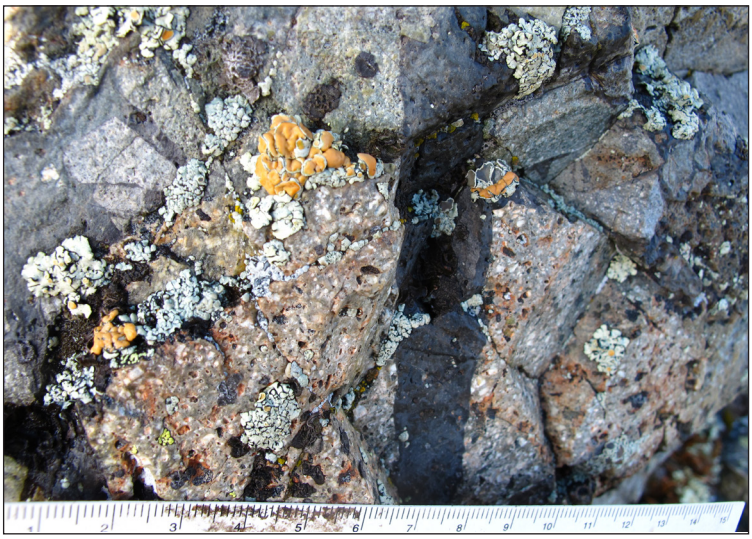

Figure 15. *Close-up of the edge of granitic clasts in dark, fine-grained andesitic matrix. A clast from this location is dated at 105.2±0.5 Ma. 373080E 6889173N; MK 060.*

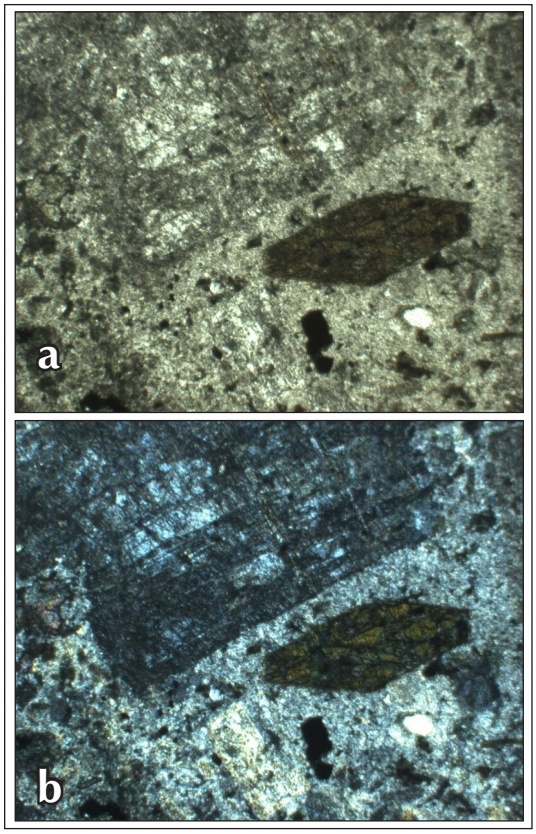

Figure 16. *Microphotographs showing euhedral amphibole, sericitized plagioclase and groundmass in altered granitic clast from breccia with andesitic matrix. Width of view: 3.0 mm: a) plane illumination and b) crossed polarized on bottom. 373080E 6889173N; MK 060.*

felsic, basaltic or ultramafic rock types, were locally observed. Fragments of metamorphic rock occur in the stratigraphically lowest breccia unit, but are not observed in higher ones.

Two 5-cm diameter clasts of porphyritic andesite (samples LM401C1 and LM401C2) were extracted from a coarse block-and-ash breccia unit relatively low in the volcanic succession using a diamond saw. A small amount of euhedral zircon was recovered and analyzed from each clast (Fig. 4e,f and Fig. 17a,b; Appendix 1). Sample LM401C1 gave 15 overlapping concordant analyses with a weighted average $^{206}Pb/^{238}U$ age of 112.2 ± 1.8 Ma. Thirteen of 15 zircon analyses from sample LM401C2 gave overlapping concordant analyses with a weighted average $^{206}Pb/^{238}U$ age of 115.2 ± 1.7 Ma. These ages are interpreted to be the crystallization ages of the two andesite clasts. These are among the oldest ages obtained from volcanic rocks of the MNVC, and provide a minimum age on the start of volcanism in the region. Two zircon grains from the second sample gave ages of 199.4 and 217.8 Ma and are interpreted to have been xenocrysts entrained from Late Triassic-Early Jurassic intrusive rocks that the andesitic magma passed through prior to eruption.

The origin of the andesitic breccia units is interpreted from observed textures. Breccia can form in vents of andesitic stratovolcanoes by repeated eruptions, dislodging previously solidified lava; this subvolcanic class includes both collapse and semi-intrusive mechanisms (Walker, 1982, p. 403). Such breccia commonly contains clasts of limited compositional range, and is likely to have restricted extent. In contrast, polylithic fragmental deposits at Mount Nansen are laterally extensive. They are interpreted as 'block–and-ash flows', and clasts locally show crude size stratification with an ash-size matrix. Clasts were likely derived from earlier formed breccia and lava flows on gravitationally unstable flanks of the volcanic edifice. The absence of bedding or sorting is consistent with a non-marine depositional setting (Francis *et al.*, 1974; Fisher and Schmincke, 1984).

Felsic flows and breccia

Rocks of map unit Ff are light pink, buff or brown weathering, and grey to black on fresh surfaces. Much of this unit appears to be massive and exposures contain up to 30% phenocrysts (or crystal fragments) of alkali feldspar and/or quartz. Bands and streaks distinguished by alternating shades of grey or brown are common and are interpreted to represent flow banding during emplacement of the volcanic unit (Fig. 18). The formerly glassy nature of the rock is revealed by spherulitic devitrification textures (Fig. 19). However, on weathered surfaces and locally in fresh surfaces dark ragged pumice and quartz and feldspar phenocrysts are present. Siliceous clasts are also visible in some outcrops, demonstrating that at least some of the unit is fragmental. The general distribution of fragmental facies appears mainly in the southwest quadrant of the volcanic complex, whereas lava flows predominate in the northeast.

A sample of grey massive rhyolite (sample MK371) collected near the centre of the Mount Nansen area was dated using U-Pb zircon methods (Fig. 17c,d; Appendix 1). Eighteen of 20 zircon grains give concordant analyses with a weighted average $^{206}Pb/^{238}U$ age of 107.4 ± 0.7 Ma, which is interpreted as the emplacement age of the rhyolite unit. One grain has minor post-crystallization Pb-loss and it was excluded from the weighted average age, and a second grain gave an older age of 164.5 Ma and is interpreted to have been a xenocryst. Mauve-grey felsic volcanic rock collected by D.J. Tempelman-Kluit on Klaza Mountain, 20 km north of Mount Nansen, provided a 109 ± 3 Ma K-Ar age (Stevens *et al.*, 1982), and is tentatively correlated with the felsic volcanic unit at Mount Nansen.

Extrusion of small volumes of rhyolitic lava commonly produce domal accumulations of limited lateral extent, whereas larger volumes may lead to the formation of a felsic flow, which has basal vitrophyre and flow layering, but lacks abundant lithic and pumice fragments (Bonnichsen and Kauffman, 1987). In the Mount Nansen area where mostly rubble is present we could not determine the overall morphology of the unit or confidently identify rapid thickness changes. Conical mounds of rubble atop ridges may be relics of domes at the appropriate erosion level, or (more likely) the site of plugs that are more resistant than their enclosing fragmental wall rock.

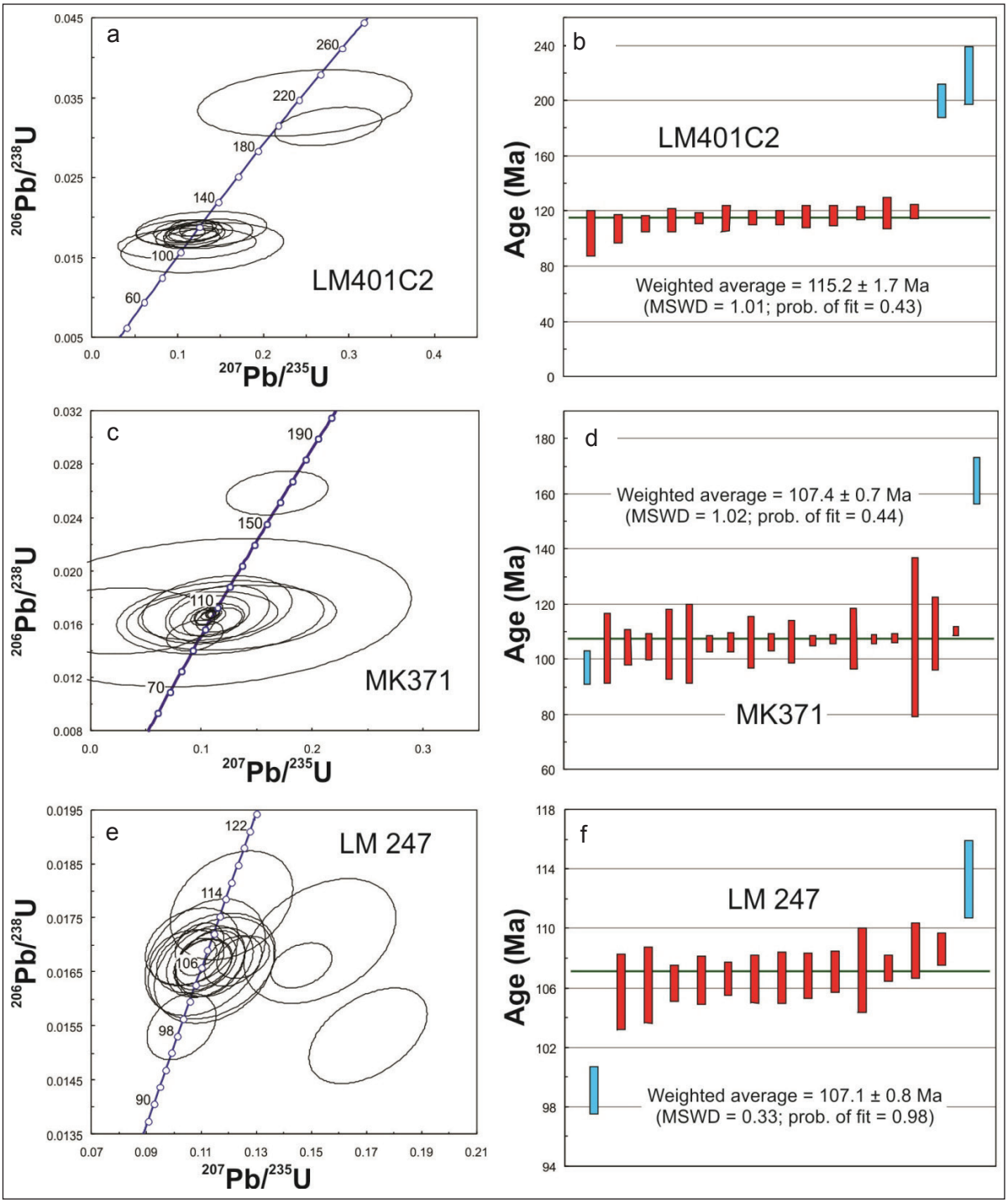

Figure 17. *U-Pb concordia diagrams and weighted average $^{206}Pb/^{238}U$ age summary plots for: a, b) LM401C2 (andesite clast in breccia), c, d) MK371 (massive rhyolite) and e, f) LM247 (granodiorite of the Dawson Range batholith). Analytical results are in Appendix 1; those shown as blue bars are excluded from the weighted average age calculation. All errors are shown at the 2σ level.*

Felsic tuff

The lithology designated as map unit Ft is characterized by a light grey, very fine grained matrix. A pronounced sub-horizontal fabric in some exposures in the southwestern part of the study area is interpreted to result from flattening (welding) of the pumice around lithic fragments and phenocrysts while still hot (ash-flow breccia; Fig. 20). Bands of melt and iron oxide particles locally crosscut fractured crystals of quartz and alkali-feldspar (Fig. 21).

Figure 18. *Full thin-section photograph of felsic rock showing convoluted flow banding, fractured quartz (white) and devitrified lithic fragments (dark). Width of view: 7.1 mm; plane-polarized illumination. 375394E 6886312N; MK 148.*

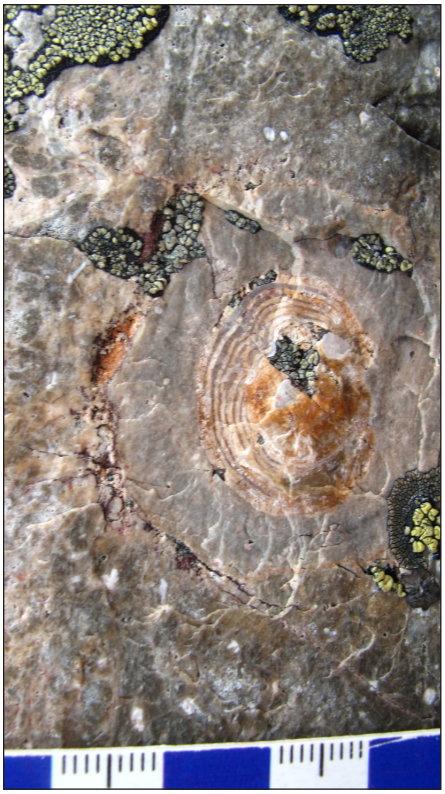

Figure 19. *Spherulitic texture indicating devitrification of a formerly glassy felsic flow. 374101E 6888867N; locality 11.*

Figure 20. *Felsic pyroclastic breccia: with ragged, flattened pumice shards (dark), feldspar crystals (white) and lithic fragments in a crystal rich ash matrix. The texture is indicative of subaerial deposition while hot. 375366E 6885552N; LM 475.*

Based on where unit Ft was encountered during mapping traverses, the outcrops and rubble of this unit form a discontinuous, laterally extensive belt ranging from a few metres thick east of Mount Nansen, to at least 150 m thick on a northern ridge spur (Fig. 3). Exposed at the head of two south flowing drainages it is at least 40 m thick. The cream weathering rubble derived from this tuff layer is evident as a band across slopes of ridge spurs west of Mount Nansen (Fig. 22). Flow banding in the unit generally dips gently and, because outcrops are found at approximately the same elevation on adjacent spurs, the unit is considered to represent sub-horizontal tuff units. Whether singular or multiple units are present could not be determined.

Epiclastic breccia

These breccia units contain a variety of clast compositions, from cherty-looking felsic to porphyritic andesite. Clasts are relatively densely packed in a lithified mud or ash-matrix (Fig. 23). A sedimentary origin for at least some of the breccia units is indicated by grains of probable detrital origin and size-sorted laminations.

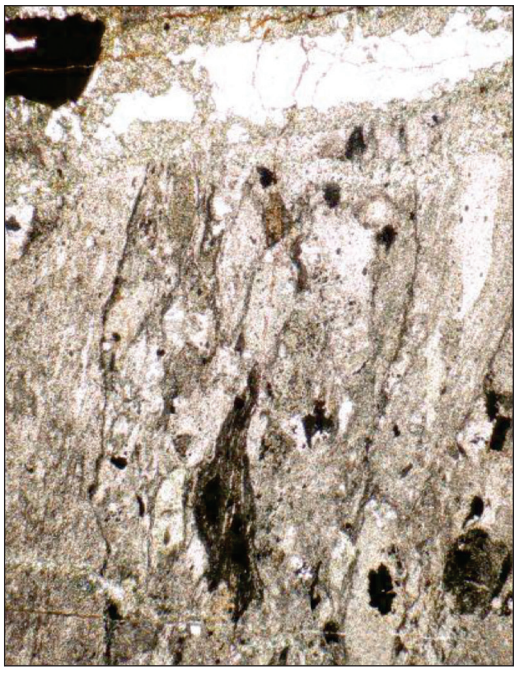

Figure 21. *Photomicrograph of felsic tuff showing ragged pieces of devitrified pumice (dark) oriented and deformed quartz (light) and lithic fragments. The thin dark lines are stylolites suggesting hydrous silica dissolution from matrix. A secondary quartz veinlet is at right. Width of view: 3.0 mm; plane-polarized illumination. 378146E 6887907N; LM 493.*

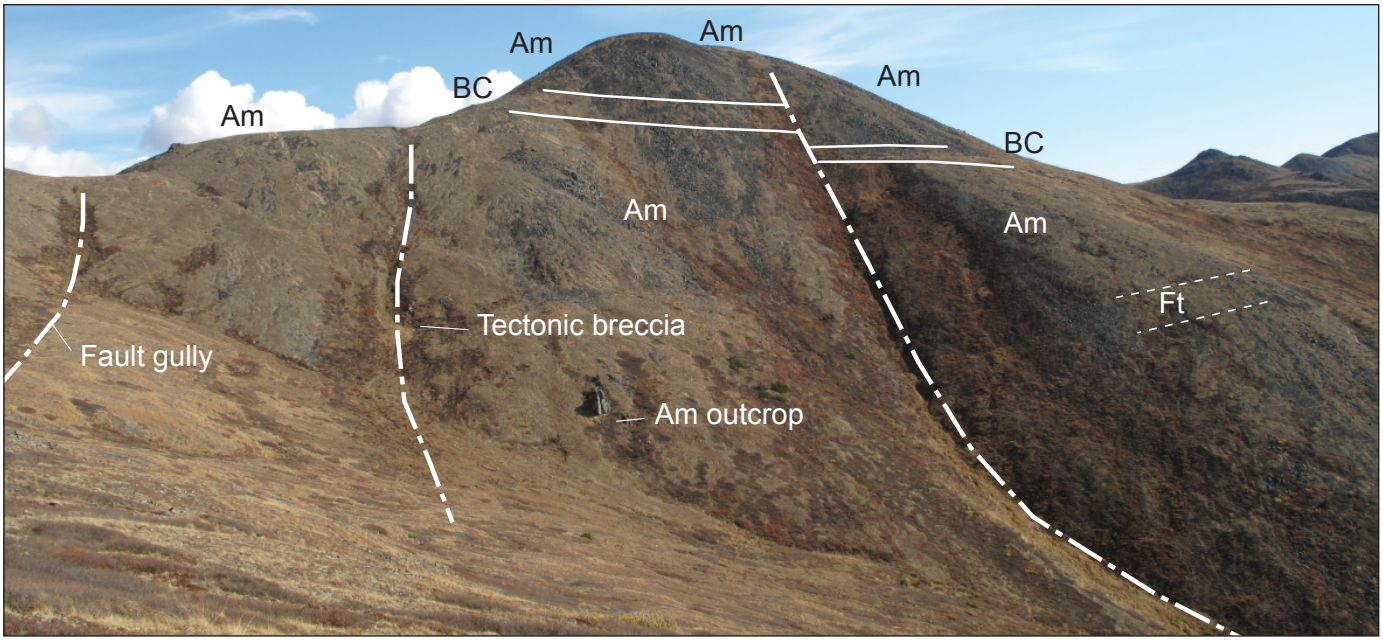

Figure 22. *View northeast toward Mount Nansen reveals a fault-offset felsite sill (BC) in massive andesite (Am) locally underlain by felsic tuff (Ft); photographed from 378400E 6888010N.*

A distinctive breccia contains mud to sand-sized particles in a hematitic or jasper-matrix (Fig. 24). The red color may stem from oxidation by air or steam. During mapping we found this distinctive breccia atop 'tors' (isolated outcrops rising above the felsenmeer). Its origin by paleo-erosion suggests that its presence marks an unconformity surface (*see* later discussion). Carlson (1987) reported this unit forming a local marker that can be traced several hundred metres across rubble slopes in the southwestern quadrant of the MNVC.

Figure 23. *Subrounded, clast supported epiclastic breccia. On the yellow scale card, black rectangles are 1 cm long. 379818E 6888040N; MK 227.*

Intrusive rocks (syn and post-volcanic)

Abundant planar, near-vertical dikes are observed cutting the volcanic units. In addition to the dikes, a sill of granite and plugs (inferred from distribution in rubble patches) of quartz-feldspar rhyolite porphyry are also present. The dikes and sills vary in composition and phenocryst type. Compositionally, the leucocratic granitic intrusions are similar to mineralized felsic stocks southeast and northeast of Mount Nansen that were described by Hart and Langdon (1998) and Mortensen *et al.* (2003; 2016). The Dawson Range batholith, exposed along the north side of the volcanic sequence, is the likely source of granitic dikes. Carlson (1987, p. 35) speculated: "Either the granodiorite intruded and partly engulfed its own earlier volcanic products, or

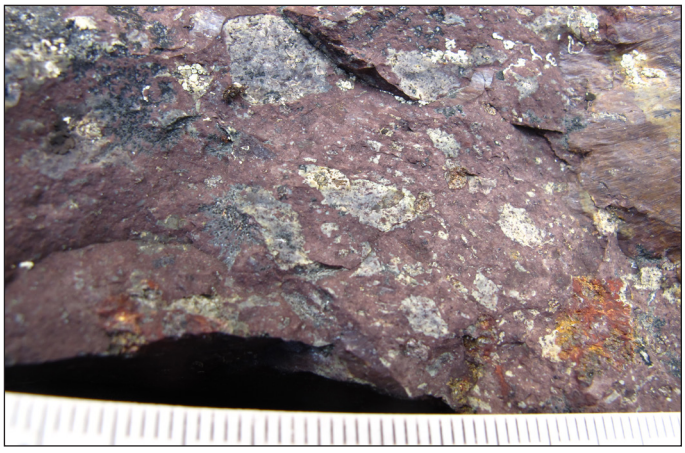

Figure 24. *Epiclastic breccia consisting of mixed felsic and andesitic clasts in maroon mud matrix. Scale graduations are mm. 376265E 6887504N; MK 005.*

the volcanic rocks were erupted through, and subsequently collapsed back into, a freshly cooled granodiorite pluton derived from a secondary magma chamber".

Here we describe five intrusive rock types in the study area; their relative ages can be deduced from crosscutting relationships, although these are difficult to confirm in areas of sparse outcrop and felsenmeer. Four new U-Pb zircon age determinations provide absolute ages for the sampled units, and the results may be extrapolated to other intrusive bodies of similar composition and/or orientation (although we cannot be sure that each comprises a single phase).

Dawson Range batholith

Mesocratic, coarse to medium-grained, equigranular hornblende biotite granodiorite (Fig. 25) is exposed on ridge spurs extending north of Mount Nansen, where its composition varies between granodiorite and monzogranite according to alkali feldspar abundance. Mafic minerals (typically hornblende > biotite) make up ~15 % of the rock by volume. Plagioclase shows distinct compositional zoning (Fig. 26).

The largest and northwestern-most representative of the Whitehorse plutonic suite (Gordey and Makepeace, 2003; Colpron, 2011) is the Dawson Range batholith. The batholith was previously separated into the Klotassin, Coffee Creek and Casino suites by Tempelman-Kluit (1984) based upon mineralogical distinctions. Minor phases, such as the Bow Creek granite (Carlson, 1987) were also identified. Precise U-Pb zircon geochronology, however, reveals that the ages of these phases overlap (Breitsprecher and Mortensen, 2004), and are all broadly contemporaneous with plutons that were grouped in the Whitehorse-Coffee Creek plutonic suite (Mortensen *et al.*, 2000; Gordey and Makepeace, 2003). Except where reset by a Late Cretaceous thermal event, many previously reported K-Ar and Rb-Sr dates for the batholith appear to be reliable (Breitsprecher and Mortensen, 2004), and generally fall in the 105-108 Ma range.

Figure 25. *Mesocratic, coarse to medium-grained, equigranular hornblende biotite granodiorite of the Dawson Range batholith. Scale in cm. 375468E 6890254N; LM 247.*

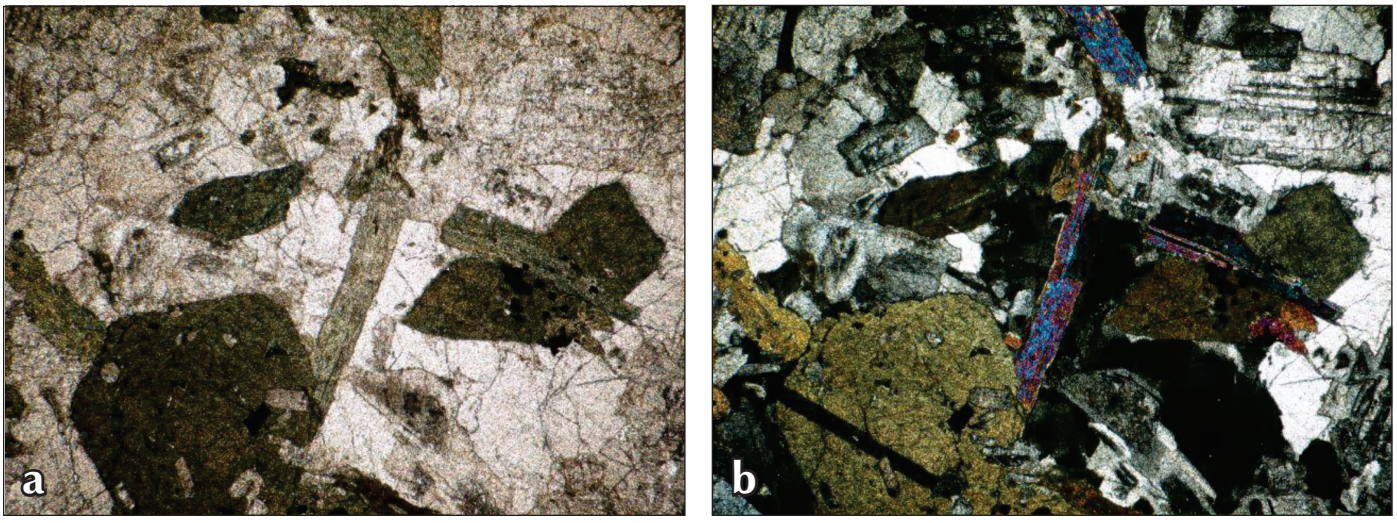

Figure 26. *Thin section of granodiorite reveals prismatic hornblende and interlocking plagioclase crystals, with 1-2 mm domains of quartz, accessory biotite (bi-refringent crystal at centre, seen edge-on) and apatite? (upper left, with high-relief). a) plane light and b) crossed-polars. 375468E 6890254N; LM 247.*

Zircons from granodiorite (sample LM247) on a spur north of the west end of the main exposure area of MNVC were separated and dated. Twenty zircon grains were analyzed (Fig. 15e,f; Appendix 1). Five of these analyses plot somewhat to the right of concordia, presumably reflecting a minor analytical problem, and were excluded from the interpretation of the results. Thirteen of the remaining 15 analyses yielded overlapping concordant analyses with a weighted average $^{206}Pb/^{238}U$ age of 107.1 ± 0.8 Ma, which is interpreted as the crystallization age of the intrusion. One grain gives a significantly younger age due to minor post-crystallization Pb-loss, and a final grain gives a somewhat older age (113.3 Ma), which is interpreted as a xenocryst, possibly derived from the andesite that occurs as clasts in unit Ab (*see* discussion above).

Blocks of andesite are found within a tabular, 50 m thick sill of granodiorite (near locality 7 on Fig. 3). Also observed are granodioritic veins splitting the andesite, confirming the intrusive relationship (Fig. 27).

Leucogranite

Plugs, dikes and veins of leucocratic monzogranite intrude the Late Triassic granite on a ridge spur 5 km south of the Mount Nansen peak. The rock contains abundant equant quartz and plagioclase in a grey or locally pink groundmass partly obscured by iron oxide alteration (Fig. 28). Hornblende phenocrysts constitute *ca.* 10% of the rock; these have a blocky aspect and crossed prisms are common. This unit is correlated with Carlson's felsic porphyry (fp) described as intruding Dawson Range Batholith northeast of Mount Nansen peak.

Figure 27. *Granitic veins intrude massive andesite. 373689E 6889191N; MK 066.*

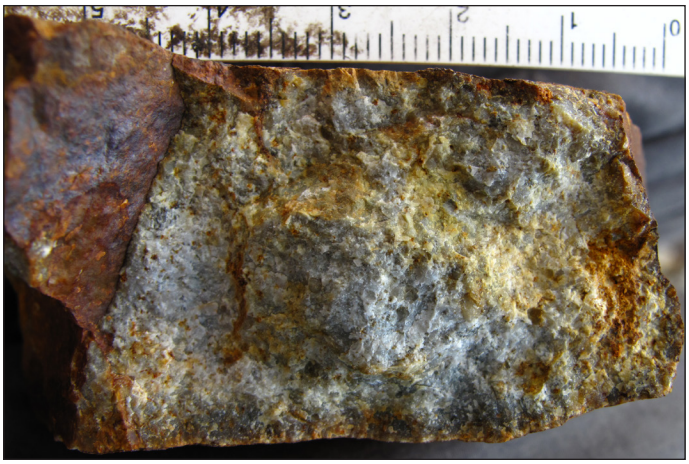

Figure 28. *Coarse-grained leucogranite consisting of white feldspar and chloritized hornblende. From ridge 4 km south of Mount Nansen, near locality 25. 378259E 6885237N; MK 306.*

Subvolcanic rock types within the MNVC

Dawson Range batholith, 5 km northwest of Mount Nansen, is cut by a variety of dikes. Three dark, glassy and fine-grained porphyritic dacite dikes, each ~3 m wide, intrude the granodiorite several hundred metres beyond the northern limit of the volcanic exposures. Dikes of similar composition intrude the volcanic rocks and the underlying basement schist. They contain a variety of phenocrysts, including ~1 cm plagioclase and lesser alkali feldspar, equant quartz and clusters of prismatic hornblende with local chlorite alteration and secondary pyrite (Fig. 29a,b). The fine-grained groundmass is typically dark on fresh surfaces and thin-sections reveal plagioclase microlites. Considerable resorption of quartz phenocrysts (Fig. 29c) indicates disequilibrium of the groundmass with earlier formed crystals. An andesitic dike within the granodiorite near the edge of the Dawson Range batholith is texturally distinguished by its acicular hornblende. Some of these northern dikes are interpreted by Carlson (1987) as possibly being younger (*e.g.*, Carmacks Group age; ~70 Ma).

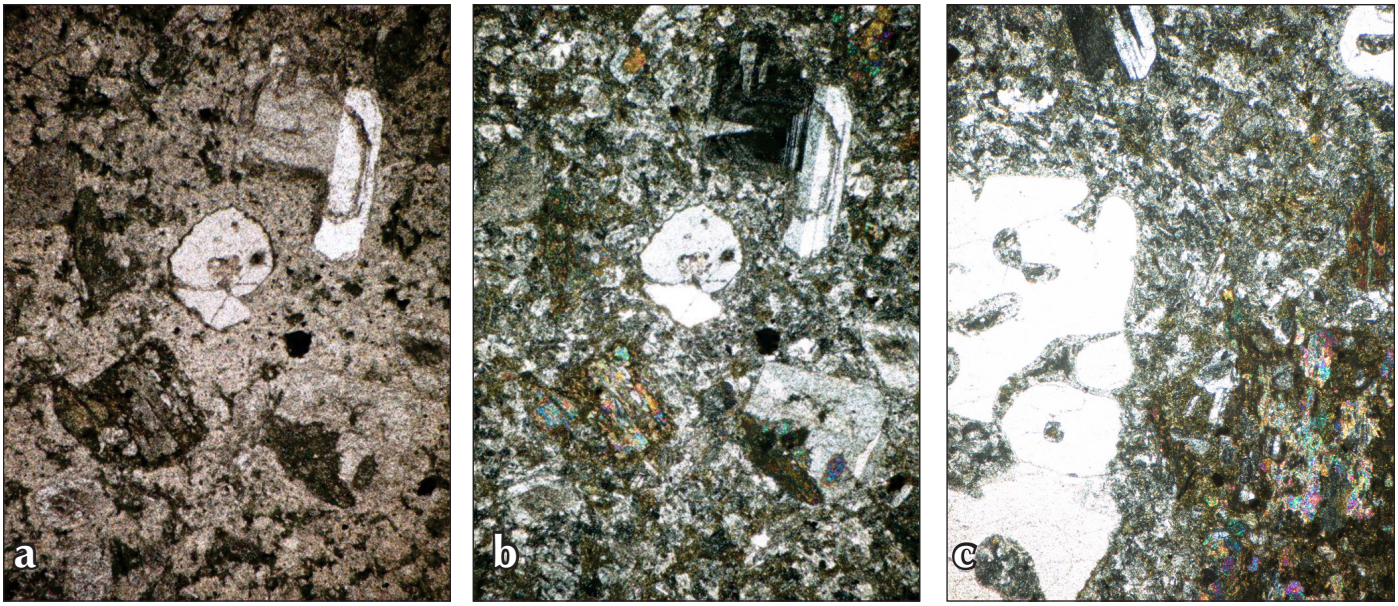

Figure 29. *Thin-section photographs of a dacite dike 7 km west-northwest of Mount Nansen: a, b) rounded quartz and alkali feldspar phenocrysts; and c) partly resorbed quartz phenocryst at right [Plane-light at left, polarized in centre and right]. Width of view in each is 3.0 mm. 375478E 6889761N; LM-223.*

Zircons from a sample of one of the dacite dikes (sample LM223A2) were separated and dated. Nineteen of 20 zircons give concordant results with a weighted average $^{206}Pb/^{238}U$ age of 105.9 ± 0.4 Ma (Fig. 30a,b; Appendix 1), indicating that this dike is only slightly younger than the main Dawson Range batholith. One grain gives a slightly younger age, reflecting minor post-crystallization Pb-loss.

Andesitic intrusions

Andesite devoid of flow features or clasts was observed around the summit of Mount Nansen (locality 15). This is interpreted as a laccolith (map unit Ai). A similar homogenous andesite porphyry was also observed with less extensive outcrop 7 km west-southwest of the summit (locality 18). This occurrence coincides with an outlier of increased magnetic response in the regional aeromagnetic survey. Although field evidence is lacking, we suggest that this andesitic body intrudes through country rock.

Felsite (BC)

Beige to pink-weathering, leucocratic alkali feldspar quartz syenite dikes (Fig. 31) are northeast-trending in the northern half of the complex. Another occurrence west of the summit of Mount Nansen is a probable sill. These contain 10% phenocrysts of sericitized alkali feldspar up to 2 mm long, together with plagioclase and biotite in a microcrystalline groundmass. Some hornblende phenocrysts are locally aligned, but no quartz phenocrysts are noted. Eighteen zircons extracted from a sample of the syenite (sample LM484) yielded a U-Pb age of 104.7 ± 0.8 Ma (Fig. 30c, d; Appendix 1). Two grains gave older ages (177.3 and 183.1 Ma) and are interpreted to have been xenocrysts.

The distinctive colour and mineralogy of this unit resembles the intrusion at Bow Creek (10 km north of

Figure 31. *Felsite intrusive rock displays distinctive pinkish grey weathering surfaces and contains alkali feldspar phenocrysts. Its texture and composition is consistent with the Bow Creek phase (Carlson, 1987) of Dawson Range batholith. Scale in mm. 375478E 6889761N; LM 441.*

Mount Nansen). Carlson's (1987) K-Ar date of ~60 Ma for the Bow Creek granite is interpreted as a reset age by Breitsprecher and Mortensen (2004). A U-Pb zircon age of 106.3 ± 0.3 Ma was obtained from a sample of the Bow Creek granite (Mortensen and Hart, unpub. data), which is now considered to be a minor phase of Dawson Range batholith.

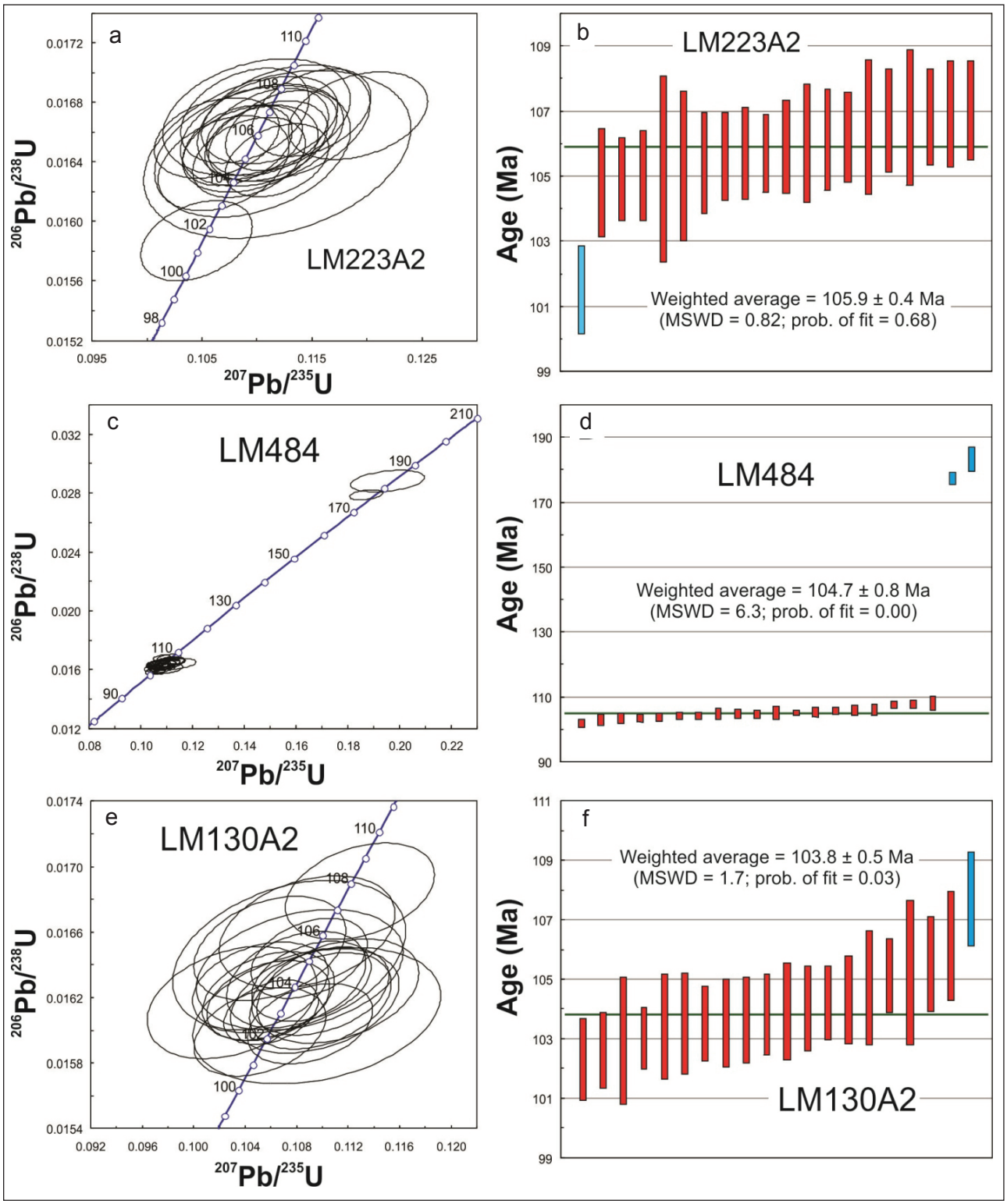

Figure 30. *U-Pb concordia diagrams and weighted average $^{206}Pb/^{238}U$ age summary plots for: a, b) LM223A2 (andesite dike), c, d) LM484 (porphyritic felsic intrusion) and e, f) LM130A2 (porphyritic granodiorite dike). Analytical results are in Appendix 1; those shown as blue bars are excluded from the weighted average age calculation. All errors are shown at the 2σ level.*

Granophyric dikes

These dikes trend northeast (050-070°), as revealed by 10-30 m wide bands of light-colored felsenmeer. The dikes also cut the Dawson Range batholith north of Mount Nansen. The few outcrops comprise fine-grained monzogranite with rounded quartz and feldspar phenocrysts up to 0.5 cm in diameter, and hornblende phenocrysts up to 1 cm long (Fig. 32). The hornblende phenocrysts are locally replaced by chlorite and contain abundant feldspar inclusions. The rock typically has a grey or locally pink groundmass and densely packed phenocrysts (Fig. 33) that may have resulted from remobilization of filter-pressed crystal mush compositionally similar to the Dawson Range granodiorite.

Zircons from a sample of this rock (sample LM130A2) yielded a U-Pb zircon age of 103.8 ± 0.5 Ma, based on a weighted average $^{206}Pb/^{238}U$ age (Fig. 30e, f; Appendix 1).

Rounded quartz porphyry

These dikes trend east and north-northwest, producing light beige-weathering streaks in felsenmeer 5 to 20 m wide. Rounded quartz and equant alkali feldspar phenocrysts are widely distributed in a pink to brown, alkali feldspar-rich groundmass (Fig. 34). These are the youngest known dikes cutting the volcanic rocks, although their relationship to the northeast trending granophyric set is locally ambiguous. They appear to feed the felsic porphyry plugs.

STRUCTURE

The andesitic units dominate the volcanic complex, whereas felsic tuffs and flow are volumetrically minor and occur primarily on topographic high points. The stratigraphically uppermost units produce plateaus and bench-like topography on slopes, suggestive of relatively planar contacts and low primary dip angles (Fig. 35). The orientation of topographically lower units is difficult to ascertain, and some possible flow contacts are observed to be inclined up to 40°. All units are cut by steep faults; hence it is possible that block rotation has affected the volcanic layering in some areas. Although the uppermost flow units have gentle dips we cannot unambiguously distinguish paleo-slope from the possibility that the entire volcanic rock package was tilted southwestward, possibly by intrusion of the underlying Dawson Range batholith.

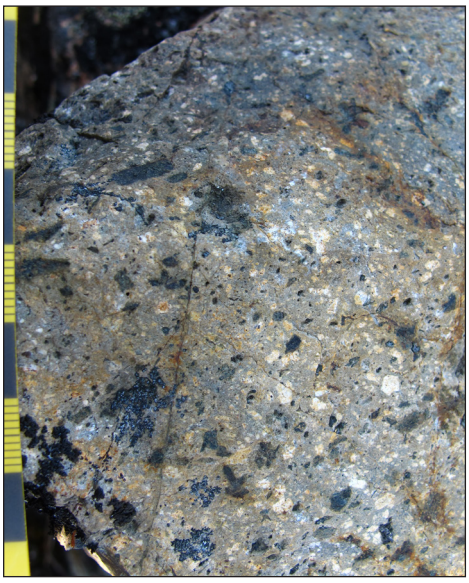

Figure 32. *Granophyric rock with blocky feldspar, rounded glassy quartz and prismatic hornblende with abundant quartz(?) inclusions, in felsic matrix. 376673E 6888367N; MK 157c.*

Figure 33. *Granophyric dike showing plagioclase and hornblende crystals densely packed within a grey felsic ground mass, possibly the result of 'filter-pressing' removal of the volatile constituents. 380969E 6888128N; LM 496, near MK 198.*

Figure 34. *Rounded quartz porphyry dike-rock; part of a north-northwest trend. 376378E 6887446N; LM 008.*

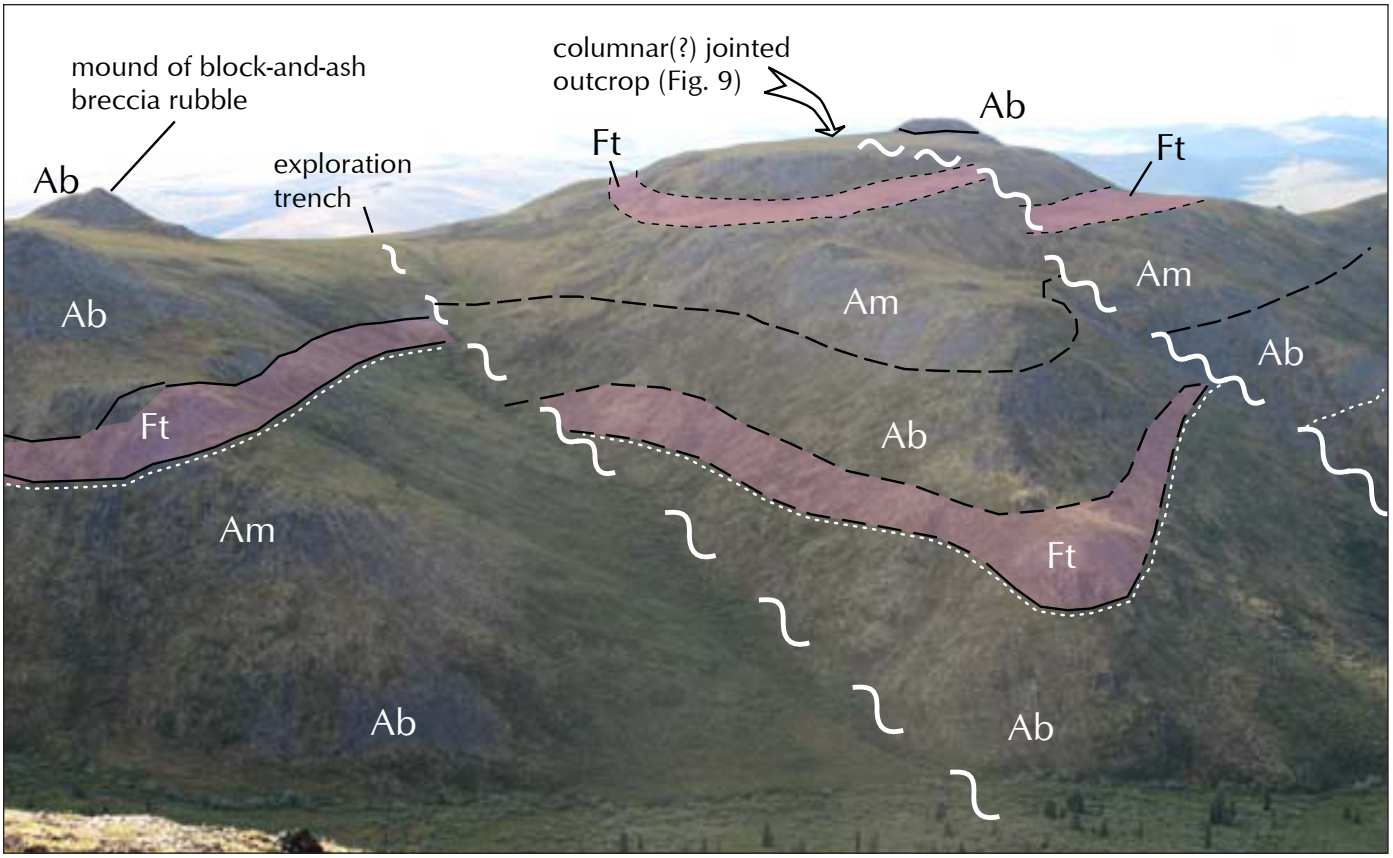

Figure 35. *Differential erosion of andesite and felsic tuff (tinted) units produces plateaus and ledges on spur ridges; vertical offset occurs across the gullies, suggesting that they are underlain by steep faults. View southwesterly from about 375000E 6887000N, to the area of locality 21.*

Faults

In areas where volcanic units are sub-horizontal, vertical offset is more easily distinguished than lateral displacement. Observed and deduced offset of map units indicate that faults likely underlie some linear gullies in the study area, some of which trend across slopes and valleys (*i.e.*, the depressions are not of hydrological origin). Sheared and crushed rock zones are observed along some inferred fault traces. Two trends of pervasive faults cut the MNVC (Fig. 3).

North-northwest-trending faults

A series of north to northwest trending faults typically show significant offset, as described by Saager and Sinclair (1974). Brittle tension gashes are observed to indicate dextral movement. The northwest-most of these faults displaces the presumed gently dipping contact between the Dawson Range batholith and MNVC volcanic rocks. It is possible that the fault is synvolcanic, and was active after extrusion of the andesite to the north, but before deposition of the felsic tuff.

Hart and Langdon (1998) recognized northwest trending structures as the defining feature of the Mount Nansen mineral trend. They interpreted mainly right lateral movement but also inferred significant vertical displacement, which created a large fault horst prior to mineralization (coincident with felsic porphyry intrusion and wall rock alteration). Subsequent lateral movement on these northwest trending structures is indicated by slickensides along veins and dikes. Mineralized porphyry dikes along some of these structures have been dated at ~108 Ma (Mortensen *et al.*, 2003, 2016). If consistent, these faults must have formed relatively early in the development of the MNVC, and should pre-date emplacement of the upper succession and dikes that cut it. The northwest-trending faults likely resulted from a pre to syn-volcanic stress regime.

Early Late Cretaceous (78-72 Ma) felsic dikes were emplaced into similar northwest-trending faults in the Klaza area, 8 km east-northeast of Mount Nansen. These faults also host the main precious and base metal veins in the Klaza deposit, which are locally strongly brecciated and are interpreted to be temporally associated with the dikes. At least some amount of younger (early Late Cretaceous or younger) displacement has therefore occurred on some of the northwest-trending faults.

Northeast-trending faults

A secondary structural trend is defined by a series of northeast striking fractures between 005° and 045° azimuth, and commonly contain quartz veins. Hart and Langdon (1998) recognized this fracture set 7 km east of Mount Nansen. There, ore pods (called "blowouts") occur where this fracture set intersects the primary northwest-trending vein-faults. In the Klaza area, significant northeast-trending faults produce both minor dextral and sinistral apparent offsets of the veins that were emplaced along the northwest-trending faults (Wengzynowski *et al.*, 2015; Ross *et al.*, 2016).

A major north-trending fault 1 km west of Mount Nansen intersects the northeasterly set. It forms a rusty notch crossing the ridge but the fault trace is covered by alluvium and vegetation.

The northeast trending faults resulted in small dextral and southeast-side down offset of the northwest-trending set (*e.g.*, Fig. 22) consistent with the sense of motion indicated by Sawyer and Dickinson (1976) and Andersen and Stroshein (1998). These faults are parallel to hornblende-phyric felsic dikes. Hart and Langdon (1998) observed a minor offset of the mineral trend and suggested that the faults originated by oblique extension to strike-slip motion of the northwest trending system.

Hart and Langdon (1998) concluded that the MNVC is a down-faulted block. However, a straight northeastern boundary of this block does not exist because the volcanic/granite contact is irregular in plan, and appears in part to reflect the current level of erosion. Furthermore, near its northwestern edge, granodiorite of the Dawson Range batholith clearly intrudes the volcanic complex as both a sill and as granitic dikes within the andesite. A graben structure was therefore not required to preserve the volcanic remnant.

LITHOGEOCHEMICAL STUDY

Sixteen samples, considered to be representative of the main intrusive and extrusive phases in the Mount Nansen area, were analyzed for major, trace and rare earth element compositions. Whole rock geochemical analyses were done at the ALS Canada laboratories in North Vancouver, BC. Selected hand specimens were first carefully trimmed of all weathered or altered surfaces using a diamond saw. Major element concentrations were determined using ICP-AES method ICP-06, and trace and rare earth element concentrations were measured using ICP-MS method MS-81. Complete analytical data are reported in Appendix 2.

The main intrusive phases (including the Late Triassic intrusion – sample LM370) in the study area, and dike rocks that cut them, range from diorite to granite in composition on a total alkalis *vs.* silica plot (Fig. 36a), and fall within the subalkaline field (Fig. 36b). On an immobile element ratio plot (Fig. 36c) all but two of the intrusive and dike samples that were analyzed cluster in the diorite to quartz diorite/granodiorite fields. This suggests that at least some of the samples that fell in the granodiorite or granite field in Figure 36a have likely experienced some degree of silicification. Intermediate volcanic rocks of the MNVC are basaltic andesite to andesite in composition, as indicated by major element (Fig. 36b) and immobile element ratios (Fig. 36d). The single MNVC sample of massive rhyolite analyzed (sample MK371) plots as a high-silica rhyolite in terms of major element composition (Fig. 36b) but as a rhyodacite in terms of immobile element ratios (Fig. 36d), also suggesting that this sample has experienced silicification after emplacement. All of the MNVC extrusive rocks fall in the subalkaline field (Fig. 36b).

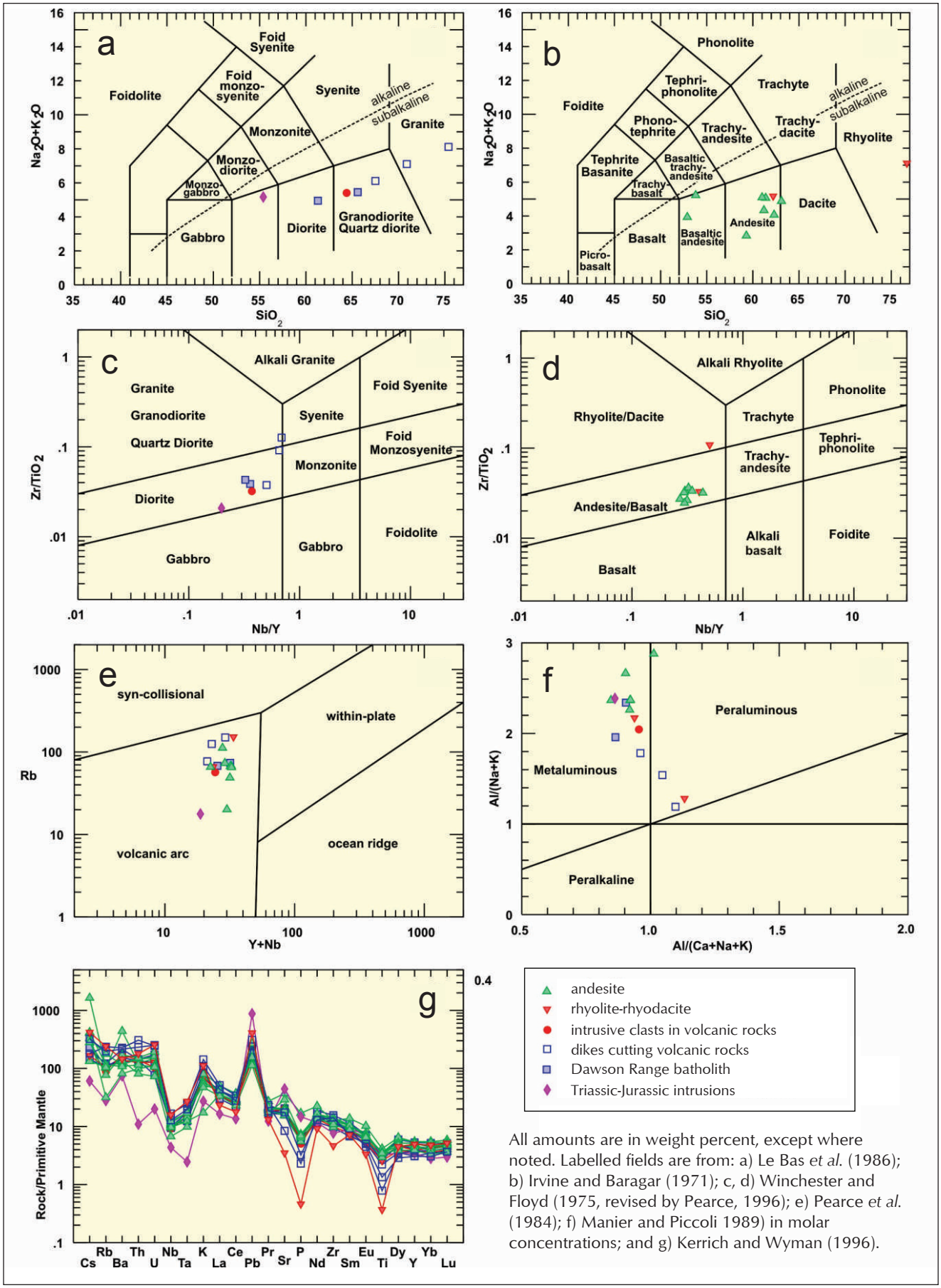

All amounts are in weight percent, except where noted. Labelled fields are from: a) Le Bas *et al.* (1986); b) Irvine and Baragar (1971); c, d) Winchester and Floyd (1975, revised by Pearce, 1996); e) Pearce *et al.* (1984); f) Manier and Piccoli 1989) in molar concentrations; and g) Kerrich and Wyman (1996).

Figure 36. *Whole rock geochemical and petro-tectonic discriminant plots for intrusive and extrusive rocks in the Mount Nansen area, central Yukon.*

A Shand-type plot shows that most of the mid-Cretaceous intrusive and extrusive rocks of the MNVC and Dawson Range batholith in the study area, along with the Late Triassic intrusion, are metaluminous in composition (Fig. 36e). The three exceptions that fall in the peraluminous field (Fig. 36e) include MK-195A2 (monzogranite dike), MK371A (massive rhyolite) and LM484A1 (felsic dike). All of these samples show petrographic evidence of strong sericitic alteration; thus the apparent peraluminous composition is probably related to superimposed alteration rather than being a primary compositional trait.

All of the intrusive and extrusive rock units in the study area fall well within the volcanic arc field (Fig. 36f). On an extended 'spidergram' plot of rare earth and high field strength elements, normalized to primitive mantle composition (Sun and McDonough, 1989; Fig. 36g), the mid-Cretaceous igneous rocks all show similar patterns, with variable but persistent Nb and Ti troughs. This pattern is considered to be typical of magma generated in a subduction setting.

The composition of the Late Triassic intrusion indicates that it is metaluminous and was emplaced in a magmatic arc setting. This is consistent with results from the somewhat younger (Early Jurassic) components of the Triassic-Jurassic plutonic suite of the Granite Batholith and Minto Pluton to the east, which also yield predominantly metaluminous compositions (Tafti, 2005).

DISCUSSIONS

Igneous style

The MNVC was deposited atop a basement of schist, quartzite and amphibolite of the Yukon-Tanana terrane, as well as a Late Triassic monzogranite intrusion. These basement rocks had been uplifted and considerably eroded before volcanism. Although the base of the MNVC is exposed and inferred to lie at ~1300 m elevation, it is disconformable in the south and noncomformable or intrusive in the north. Furthermore, the present exposure is an erosional remnant, without indication of whether volcanic rocks once extended northeastward to connect with those preserved at Victoria Mountain, or in any other direction. Based upon our observations it is impossible to determine whether an extensive volcanic field once covered much, or all of the Dawson Range, or whether those at Mount Nansen constitute an isolated primary volcanic centre.

The attitude of volcanic rocks suggests there are at least two stages in the evolution of the volcanic edifice. Angular truncation of inclined layers inferred in several places suggests that structural disruption or depositional hiatus occurred at least once during its construction. Rocks above and below this structural discontinuity are here referred to as the 'upper' volcanic succession, and the 'lower' succession, respectively; their distribution is shown on Figure 37. Although similar rock types are present in both successions the structural discontinuity is apparent despite vertical offset by south-trending faults. The upper succession displays sub-horizontal layering west of a fault through the centre of the complex, whereas moderately dipping units predominate to the east. The steep orientation of aligned phenocrysts and flow banding also distinguish the two successions. The lower succession, comprising interbedded andesite lava and fragmental flows and local epiclastic breccia, is interpreted as remnants of an older stratovolcano, probably with satellite vents. A breccia containing andesite porphyry clasts dated 112 and 115 Ma indicates the minimum age for the oldest volcanism in this area.

The upper succession, which is at least 180 m thick, is dominated by pyroclastic deposits, ranging from andesitic block-and-ash breccia to felsic tuff, and alternating with andesite flows that vary in phenocryst content and abundance. The sub-horizontal, commonly tabular flows and relatively widespread felsic tuffs suggest a more distal environment than that indicated by the lower succession.

Crystallization ages of 105.9 Ma and 107.4 Ma for an andesite dike and a felsic tuff unit respectively in the upper succession suggest that at least some of the upper succession is no more than 9 million years younger

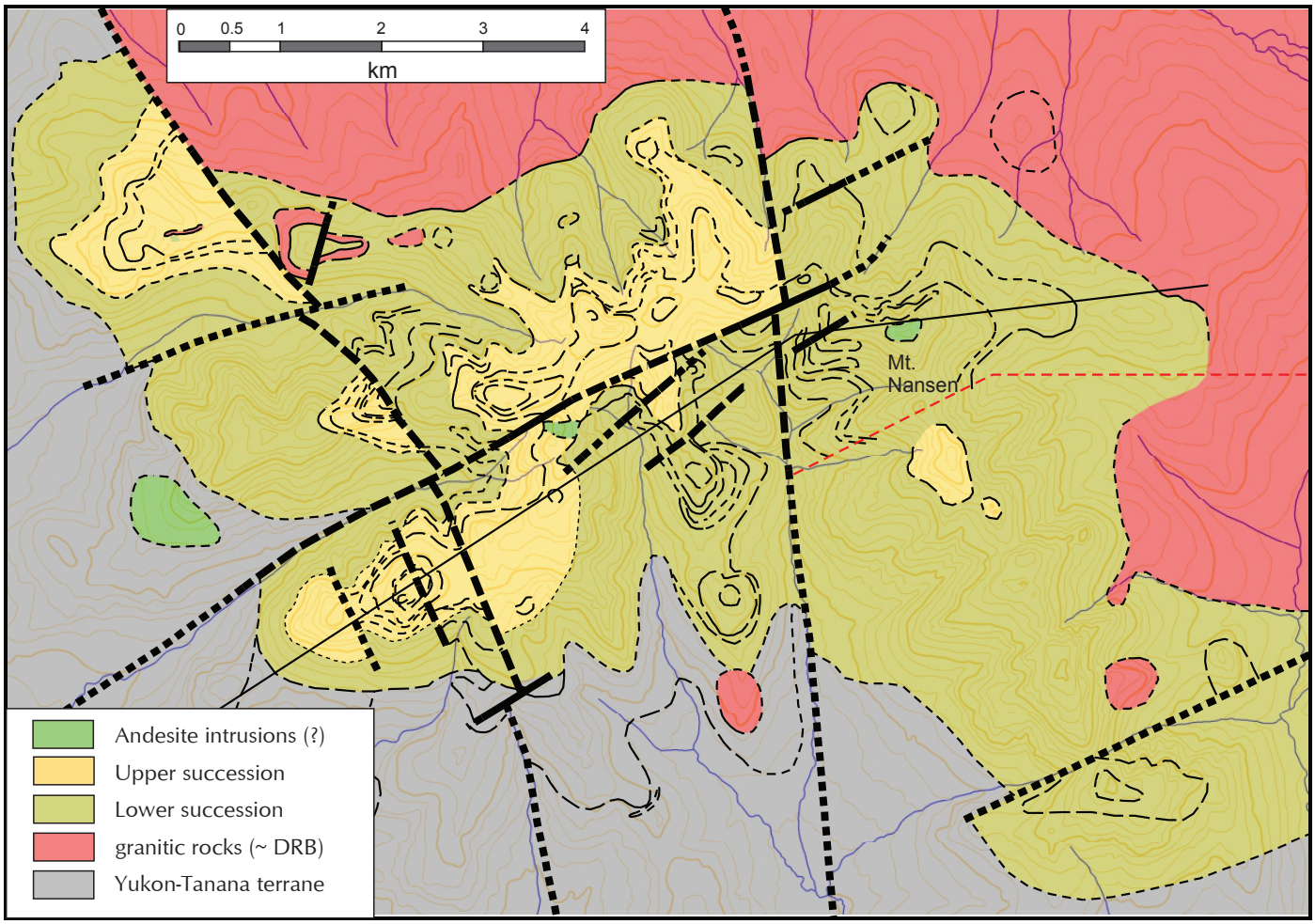

Figure 37. *General distribution of Lower (interpreted as proximal facies) and Upper (interpreted as distal facies) successions, interpreted from rock types and relationships.*

than the lower succession (Fig. 38). Differences in the orientation of primary layering between the lower and upper successions imply that at least parts of the edifice were tilted and partly eroded between deposition of the two packages. We have no information to determine whether volcanism was episodic or protracted.

Granodiorite of the Dawson Range batholith intruded into the lower succession at ~107 Ma. Rounded granitic cobbles enclosed in andesitic matrix crystallized at 105 Ma, indicating that either the granite was stoped and milled in a volcanic conduit, or part of the pluton was un-roofed by erosion prior to that time. We speculate that the intrusion of granodiorite into the base of the volcanic system likely caused tilting, differential uplift and erosion of the still relatively young volcanic complex. Dikes dated 106 and 103 Ma are aligned with, and in part occupy, sub-parallel, steep faults, and are presumed to represent the youngest phase of Mount Nansen magmatism.

Volcanic evolution

The MNVC is part of a volcanic arc built upon the tilted and deformed Yukon-Tanana and Mesozoic successor basin strata that have been accreted and overlap the Laurentian margin. The arc is the product of eastward-dipping subduction.

Beginning before 115 million years ago, a composite sub-aerial stratovolcano formed atop a relatively planar erosion surface – without standing water bodies (no textures indicative of waterlain deposition were observed). The chief volcanic products are andesitic flows and monolithologic breccia consistent with a proximal facies interpretation. This is the lower succession volcanic edifice.

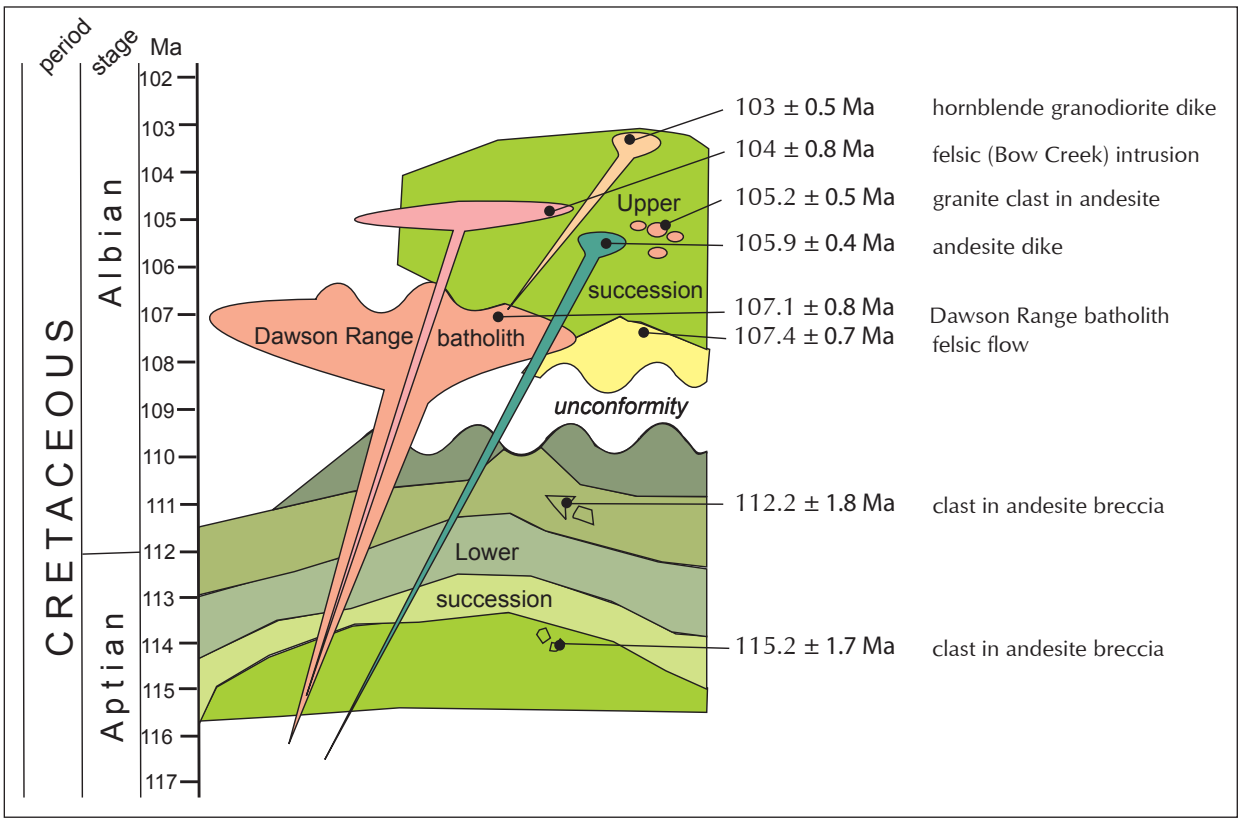

Figure 38. *Schematic diagram of age relationships based upon geochronological results in this report.*

Abundant breccia characterizes volcanoes with topographic relief; they form within the magma conduit as well as on outer slopes; mechanical erosion largely controls preservation of deposits. The sequence of eruptions and possibly collapse of summit regions modify the original landform. Although few if any steep andesite flows remain, parts of rhyolite domes and abundant breccia are present. Large volumes of monolithic, angular breccia suggest andesite lava cooled in mechanically unstable masses on steep slopes. Clast supported breccia was incorporated in the base of subsequent lava flows or remobilised on the surface; these became matrix supported deposits down slope. On present-day andesitic volcanoes, clasts can be traced to parent lavas which are topographically higher but stratigraphically lower (*cf*., Francis *et al.*, 1974); this relationship was interpreted at Mount Nansen. Poor sorting and a muddy matrix are commonly observed, but not bedding structures.

Block and ash breccia clasts may have been sourced from the walls of the vent as well as by cannibalizing earlier deposits, thus producing a variety of clast types. The older edifice was on-lapped by growth of adjacent volcano(es). An apron of pyroclastic deposits, epiclastic breccia and less common andesite flows which fill topographic lows constitute the Upper succession, and intrusions within it are 109 to 107 Ma. This distal environment may have received volcanic debris from southwest of Mt. Nansen because welded pyroclastic breccia was only observed in that area, suggesting a thicker deposit (Fisher and Schmincke 1984, p. 196).

By ~105 Ma the volcanic edifice was broken by block-faults and was intruded by the underlying batholith; this is indicated by numerous dikes and laccoliths. Mass wasting or continued eruptions are indicated by volcanic breccia that includes granitic clasts.

Until the present day the MNVC has remained a highland. Extensive areas of granodiorite indicate at least several kilometres of overlying carapace were removed, exposing the Dawson Range batholith. The volcanic rock of the MNVC is prominent because it is more resistant to erosion, thermally hardened by the underlying intrusion.

CONCLUSION

Mid-Cretaceous volcanic rocks at Mount Nansen are an erosional remnant of a predominantly andesitic arc volcanic tract that is in part underlain and intruded by the Dawson Range batholith. Volcanic exposures are interpreted to represent both vent-proximal and more distal facies; these are cut by high-level dikes that occupy sub-parallel fault sets. They are not significantly down-faulted with respect to surrounding country rock, but appear to topographically overlie and disconformably overlap older rocks.

The volcanic and plutonic rocks represent a coeval suite. Granitic clasts are incorporated into the volcanic breccia, and andesitic dikes intrude the nearby granite.

Field relationships and geochronology indicate that the Dawson Range batholith was co-magmatic with the later andesitic and felsic volcanism on Mount Nansen, whereas the oldest volcanic rocks appear to have pre-dated emplacement of the batholith. It is possible that a subsequent pulse or differentiation of the granitic magma chamber that intruded into the base of the volcano opened vertical fractures, and these hosted felsic dikes at the end of this phase of Cretaceous volcanism.

ACKNOWLEDGMENTS

This open file was distilled from independent mapping reports to fulfill a course requirement of the Earth Sciences Department at Cambridge University (Klöcking, 2012; Mills, 2012). Supervisors John Maclennan and Nigel Woodcock provided wise counsel. Fieldwork was supported by Studienstiftung des deutschen Volkes, Mary Euphrasia Mosley and Sir Bartle Frere & Worts travel funds, G.R.N. Minchin Fund and the Geological Society of London.

The first two authors studied the geologically complex Dawson Range as volunteer assistants on a regional mapping project by the Geological Survey of Canada that was carried out by Jim Ryan, Alex Zagorevski and Witold Ciolkiewicz. Helicopter access was funded by the Geological Survey of Canada and the University of British Columbia. Matt Turner and Heather Smith welcomed us at the Rockhaven Resources' exploration camp. The Yukon Geological Survey provided daily safety check-ins during fieldwork. Steve Israel made helpful suggestions to an early version, and a thoughtful review.

REFERENCES

Allan, M.M., Mortensen, J.K., Hart, C.J.R., Bailey, L.A., Sánchez, M.G., Ciolkiewicz, W., McKenzie, G.G. and Creaser, R.A., 2013. Magmatic and Metallogenic Framework of West-Central Yukon and Eastern Alaska; Chapter 4. *In*: Tectonics, Metallogeny, and Discovery: The North American Cordillera and Similar Accretionary Settings; M. Colpron, T. Bissig, B.G. Rusk, and J.F.H. Thompson (eds.), Society of Economic Geologists, Special Publication 17, p. 111-168.

Andersen, F. and Stroshein, R. (1998). Geology of the Flex gold-silver vein system, Mount Nansen area, Yukon. *In*: Yukon Exploration and Geology 1997, Exploration and Geological Services Division, Yukon Region, Indian and Northern Affairs Canada, p. 139-143.

Bacon, C.R., Foster, H.L. and Smith, J.G., 1990. Rhyolitic calderas of the Yukon-Tanana terrane, east-central Alaska. Journal of Geophysical Research, vol. 95, no. B13, p. 21,451-21,461.

Beranek, L.P. and Mortensen, J.K., 2011. The timing and provenance record of the Late Permian Klondike orogeny in northwestern Canada and arc-continent collision along western North America. Tectonics, vol. 30, no. 5, p. TC5017.

Berman, R.G., Ryan, J.J., Gordey, S.P. and Villeneuve, M., 2006. Permian to Cretaceous polymetamorphic evolution of the Stewart River region, Yukon-Tanana terrane, Yukon, Canada: P-T evolution linked with in situ SHRIMP monazite geochronology. Journal of Metamorphic Geology, vol. 25, issue 7, p. 803-827, doi:10.1111/j.1525-1314.2007.00729.

Bonnichsen, B. and Kauffman, D., 1987. Physical features of rhyolite lava flows in the Snake River plain volcanic province, southwestern Idaho. Geological Society of America, Special Paper 212, p. 119-145.

Bostock, H.S., 1936. Carmacks District, Yukon. Geological Survey of Canada, Memoir 189, 67 p.

Breitsprecher, K. and Mortensen, J.K. (compilers), 2004. YukonAge 2004: A database of isotopic age determinations for rock units from Yukon Territory. Yukon Geological Survey, CD-ROM.

Carlson, G., 1987. Bedrock geology of Mount Nansen (115I/3) and Stoddart Creek (115I/6) map areas, Dawson Range, central Yukon. Exploration and Geological Services Division, Yukon Region, Indian and Northern Affairs Canada, Open File 1987-2.

Colpron, M. (Comp.), 2011. Geological compilation of Whitehorse trough: Whitehorse (105D), Lake Lebarge (105E), and part of Carmacks (115I), Glenlyon (105L), Ashihik Lake (115H), Quiet Lake (105F) and Teslin (105C) (1:250 000 scale). Yukon Geological Survey, Geoscience map 2011-1 (3 maps, legend and appendices).

Colpron, M., Gordey, S., Lowey, G., White, D. and Piercey, S., 2007. Geology of the northern Whitehorse trough, Yukon (105E/12, 13 and parts of 11 and 14; 105L/4 and parts of 3 and 5; parts of 115H/9 and 16; 115I/1 and part of 8). Yukon Geological Survey, Open File 2007-6, scale 1:150 000.

Colpron, M., Israel, S., Murphy, D., Pigage, L. and Moynihan, D., 2016. Yukon bedrock geology map. Yukon Geological Survey, Open File 2016-1, scale 1:1 000 000, map and legend.

Colpron, M., Murphy, D.C., Nelson, J.L., Roots, C.F., Gladwin, K., Gordey, S.P. and Abbott, J.G., 2003. Yukon Targeted Geoscience Initiative, Part 1: Results of accelerated bedrock mapping in Glenlyon (105L/1-7, 11-14) and northeast Carmacks (115I/9, 16) areas, central Yukon. *In*: Yukon Exploration and Geology 2002, D.S. Emond and L.L. Lewis (eds.), Yukon Geological Survey, p. 85-108.

Colpron, M., Nelson, J.L. and Murphy, D.C., 2006. A tectonostratigraphic framework for the pericratonic terranes of the northern Cordillera. *In:* Paleozoic Evolution and Metallogeny of Pericratonic Terranes at the Ancient Pacific Margin of North America, Canadian and Alaskan Cordillera, M. Colpron and J.L. Nelson (eds.), Geological Association of Canada, Special Paper 45, p. 1-23.

Colpron, M. and Ryan, J.J., 2010. Bedrock geology of southwest McQuesten (NTS 115P) and part of northern Carmacks (NTS 115I) map area. *In:* Yukon Exploration and Geology 2009, Yukon Geological Survey, p. 159-184.

Currie, L.D. and Parrish, R.R., 1997. Paleozoic and Mesozoic rocks of Stikinia exposed in northwestern British Columbia: implications for correlations in the northern Cordillera. Geological Society of America Bulletin, vol. 109, no. 11, p. 1402-1420.

Dorsey, C., 2013. Analysis of the structure, stratigraphy and geological evolution of Canyon Mountain, Whitehorse, Yukon. Unpublished BSc thesis, University of Calgary, 58 p.

Edwards, B.R. and Russell, J.K., 2000. Distribution, nature, and origin of Neogene–Quaternary magmatism in the northern Cordilleran volcanic province, Canada. Geological Society of America Bulletin, vol. 112, p. 1280-1295.

Fisher, R. and Schmincke, H.-U., 1984. Pyroclastic Rocks. Springer Verlag, 472 p.

Francis, P.W., Roobol, M.J., Walker, G.P.L., Cobbold, P.R. and Coward, M., 1974. The San Pedro and San Pablo volcanoes of northern Chile and their hot avalanche deposits. Geologische Rundschau, vol. 63, issue 1, p. 357-388, doi:10.1007/BF01820994.

Gordey, S.P. and Makepeace, A.J., 2003. Yukon Digital Geology. Yukon Geological Survey, Geoscience Map 2003-9 (http://data.geology.gov.yk.ca/Reference/42240).

Gordey, S.P., Williams, S.P., Cocking, R.B. and Ryan, J.J., 2006. Digital geology, Stewart River area, Yukon. Geological Survey of Canada, Open File 5122, 1 DVD, doi:10.4095/221967.

Grond, H.E., Churchill, S.J., Armstrong, R.L., Harakal, J.E. and Nixon, G.T., 1984. Late Cretaceous age of the Hutshi, Mount Nansen and Carmacks groups, southwestern Yukon Territory and northwestern British Columbia. Canadian Journal of Earth Sciences, vol. 21, p. 554-558.

Hart, C.J.R., 1995. Magmatic and tectonic evolution of the Omineca superterrane and Coast Plutonic Complex in southern Yukon Territory. Unpublished MSc thesis, University of British Columbia, Vancouver, British Columbia.

Hart, C.J.R., 1997. A transect across northern Stikinia: Geology of the northern Whitehorse map area, southern Yukon Territory (105D/13-16). Yukon Geological Survey, Bulletin 8, 78 p.

Hart, C.J.R., Goldfarb, R.J., Lewis, L.L. and Mair, J.L., 2004. The Northern Cordilleran mid-Cretaceous plutonic province: ilmenite/magnetite-series granitoids and intrusion-related mineralisation. Resource Geology, vol. 54, p. 253-280.

Hart, C.J.R. and Langdon, M., 1998. Geology and mineral deposits of the Mount Nansen camp, Yukon. *In*: Yukon Exploration and Geology 1997, Yukon Geological Survey, p. 129-138.

Hart, C.J.R. and Radloff, J.K., 1990. Geology of Whitehorse, Alligator Lake, Fenwick Creek, Carcross and part of the Robinson map areas (105D/11, 6, 3, 2 and 7). Exploration and Geological Services Division, Yukon Region, Indian and Northern Affairs Canada, Open File 1990-4, 113 p. and five maps, 1:50 000 scale.

Hart, C. and Villeneuve, M. 1999. Geochronology of Neogene alkaline volcanic rocks (Miles Canyon basalt), southern Yukon Territory, Canada: the relative effectiveness of laser $^{40}Ar/^{39}Ar$ and K-Ar geochronology. Canadian Journal of Earth Sciences, vol. 36, p. 1495-1507, doi: 10.1139/e99-049.

Israel, S. and Borch, A., 2015. Preliminary geological map of the Long Lake area, parts of NTS 115H/2 and 115H/7. Yukon Geological Survey, Open File 2015-32, 1:50 000 scale.

Israel, S. and Westberg, E., 2012. Geology and mineral potential of the northwestern Aishihik Lake map area, parts of NTS 115H/12 and 13. *In*: Yukon Exploration and Geology 2011, K.E. MacFarlane and P.J. Sack (eds.), Yukon Geological Survey, p. 103-113.

Johnston, S.T., 1995. Geological compilation with interpretation from geophysical surveys of the northern Dawson Range, central Yukon (115-J/9 and 115-J/10, 115-I/12, 1:100 000 scale map). Exploration and Geological Services Division, Yukon Region, Indian and Northern Affairs Canada, Open File 1995-2(G).

Johnston, S.T. and Hachey, N., 1993. Preliminary results of 1:50 000-scale geologic mapping in Wolverine Creek map area (115 I/12), Dawson Range, southwest Yukon. *In*: Yukon Exploration and Geology 1992, Exploration and Geological Services Division, Yukon Region, Indian and Northern Affairs Canada, p. 49-60.

Johnston, S.T. and Shives, R.B.K., 1995. Interpretation of an airborne multiparameter geophysical survey of the northern Dawson Range, central Yukon: A progress report. *In*: Yukon Exploration and Geology, 1994, Exploration and Geological Services Division, Yukon Region, Indian and Northern Affairs Canada, p. 105-111.

Johnston, S.T., Mortensen, J.K. and Erdmer, P., 1996a. Igneous and meta-igneous age constraints for the Aishihik metamorphic suite, southwest Yukon. Canadian Journal of Earth Sciences, vol. 33, p. 1543-1555.

Johnston, S.T., Wynne, P.J., Francis, D., Hart, C.J.R., Enkin, R.J. and Engebretson, D.C., 1996b. Yellowstone in Yukon: The Late Cretaceous Carmacks Group. Geology, vol. 24, p. 997-1000, doi: 10.1130/0091-7613(1996)024<0997:YIYTLC>2.3.CO;2.

Klöcking, M., 2012. Bedrock Geology of Mt. Nansen, Yukon, Canada; Part II Mapping project. Department of Earth Sciences, University of Cambridge, England. 35 p. and accompanying map, (unpublished).

Lambert, M.B., 1974. The Bennett Lake cauldron subsidence complex, British Columbia and Yukon Territory. Geological Survey of Canada, Bulletin 227.

McDonald, B.W.D., 1990. Geology and genesis of the Mount Skukum epithermal gold-silver deposits, southwestern Yukon Territory (NTS 105D 3, 6). Exploration and Geological Services Division, Yukon Region, Indian and Northern Affairs Canada, Bulletin 2, 65 p.

Mihalynuk, M., Nelson, J. and Diakow, L.J., 1994. Cache Creek terrane entrapment: Oroclinal paradox within the Canadian Cordillera. Tectonics, vol. 13, p. 575–595.

Mills, L.E., 2012. The Geology of Mt. Nansen, Yukon, Canada; Part II Mapping project. Department of Earth Sciences, University of Cambridge, England. 63 p. and accompanying map (unpublished).

Miskovic, A. and Francis, D., 2004. The Early Tertiary Sifton Range volcanic complex, southwestern Yukon. *In*: Yukon Exploration and Geology 2003, D.S. Emond and L.L. Lewis (eds.), Yukon Geological Survey, p. 143-155.

Monger, J.W.H., Wheeler, J.O, Tipper, H.W., Gabrielse, H., Harms, T., Struik, L.C., Campbell, R.B., Dodds, C.J., Gehrels, G.E. and O'Brien, J., 1991. Part B. Cordilleran terranes. *In*: Upper Devonian to Middle Jurassic assemblages, Chapter 8 of Geology of the Cordilleran Orogen in Canada, H. Gabrielse and C.J. Yorath (eds.), Geological Survey of Canada, Geology of Canada, no. 4, p. 281-327.

Mortensen, J.K., 1992. Pre-Mid-Mesozoic evolution of the Yukon-Tanana terrane, Yukon and Alaska. Tectonics, vol. 11, p. 836-853.

Mortensen, J.K., Appel, V. and Hart, C.J.R., 2003. Geological and U-Pb age constraints on base and precious metal vein systems in the Mount Nansen area, eastern Dawson Range, Yukon. *In*: Yukon Exploration and Geology 2002, D.S. Emond and L.L. Lewis (eds.), Exploration and Geological Services Division, Yukon Region, Indian and Northern Affairs Canada, p. 165-174.

Mortensen, J.K. and Dusel-Bacon, C., 2014. Nature and U-Pb zircon ages of mid-Cretaceous calderas and tuffs in eastern Alaska and western Yukon: Implications for landscape evolution in the northern Cordillera. Geological Association of America, Annual General Meeting, Vancouver, BC, Oct. 21-24, 2014, paper 330-4.

Mortensen, J., Hart, C., Murphy, D. and Heffernan, S., 2000. Temporal evolution of Early and mid-Cretaceous magmatism in the Tintina Gold Belt. *In*: The Tintina Gold Belt: concepts, exploration and discoveries, J. Jambor (ed.), British Columbia and Yukon Chamber of Mines, Special Volume 2, p. 49-57.

Mortensen, J.K., Hart, C.J.R., Tarswell, J. and Allan, M.M., 2016. U-Pb zircon age and Pb isotopic constraints on the age and origin of porphyry and epithermal vein mineralization in the eastern Dawson Range, Yukon. *In:* Yukon Exploration Geology 2015, K.E. MacFarlane and M.G. Nordling (eds.), Yukon Geological Survey, p. 165-185, including appendices.

NACSN, 2005. North American stratigraphic code. American Association of Petroleum Geologists Bulletin, vol. 89, p. 1547-1591.

Nelson, J. and Colpron, M., 2007. Tectonics and metallogeny of the British Columbia, Yukon and Alaskan Cordillera, 1.8 Ga to the present. *In:* Mineral Deposits of Canada: A Synthesis of Major Deposit-types, District Metallogeny, the Evolution of Geological Provinces, and Exploration Methods, W.D. Goodfellow (ed.), Geological Association of Canada, Mineral Deposits Division, Special Publication no. 5, p. 755-791.

Nelson, J.L., Colpron, M., Piercey, S.J., Dusel-Bacon, C., Murphy, D.C. and Roots, C.F., 2006. Paleozoic tectonic and metallogenic evolution of the pericratonic terranes in Yukon, northern British Columbia and eastern Alaska, *In*: Paleozoic Evolution and Metallogeny of Pericratonic Terranes at the Ancient Pacific Margin of North America, Canadian and Alaskan Cordillera, M. Colpron and J.L. Nelson (eds.), Geological Association of Canada, Special Paper 45, p. 323-360.

Owen, D.E., 1987. Commentary: Usage of stratigraphic terminology in papers, illustrations, and talks. Journal of Sedimentary Petrology, vol. 57, p. 363-372.

Payne, J.G., Gonzales, R.A., Akhurst, K. and Sisson, W.G., 1987. Geology of Colorado Creek (115J/10), Selwyn River (115J/9) & Prospector Mountain (115I/5) map areas, western Dawson Range, west Central Yukon. Yukon Geological Survey, Open File 1987-3(G).

Roots, C.F., 1981. Geological setting of gold-silver veins on Montana Mountain. *In*: Yukon Geology and Exploration 1979-80, Exploration and Geological Services Division, Yukon Region, Indian and Northern Affairs Canada, p.116-122.

Roots, C.F., 1982. Geology of the Montana Mountain area. Unpublished MSc thesis, Carleton University, Ottawa, 127 p.

Ross, A.A., Martin, C.J. and Dumala, M.R., 2016. Technical report describing updated diamond drilling, metallurgical testing and mineral resources on the Klaza property, Yukon, Canada. Unpublished NI 43-101 technical report prepared for Rockhaven Resources Ltd., 81 p. http://www.rockhavenresources.com/assets/projects/2016-01-22_klaza_ni-43-101.pdf [accessed Feb. 21, 2016].

Ryan, J.J., Zagorevski, A., Williams, S.P., Roots, C., Ciolkiewicz, W., Hayward, N. and Chapman, J.B., 2013. Geology, Stevenson Ridge (northeast part), Yukon. Geological Survey of Canada, Canadian Geoscience Map 116, (ed. prelim.); 1 sheet, doi:10.4095/292371.

Ryan, J.J., Westberg, L.W., Williams, S. and Chapman, J., 2016. Geology of the Mount Nansen – Nisling River area, southwest Yukon. Poster, 2016 Exploration Roundup, Vancouver, BC.

Saager, R. and Bianconi, F., 1971. The Mount Nansen Gold-Silver Deposit, Yukon Territory, Canada. Mineralium Deposita, vol. 6, p. 209-224.

Saager, R. and Sinclair, A.J., 1974. Factor analysis of stream sediment geochemical data from the Mount Nansen area, Yukon Territory, Canada. Mineralium Deposita, vol. 9, p. 243-252.

Sanchez, M.G., Allan, M.M., Hart, C.J.R. and Mortensen, J.K., 2013. Orogen-perpendicular magnetic segmentation of the western Yukon and eastern Alaska Cordilleran hinterland: Implications for structural control of mineralization. *In*: Yukon Exploration and Geology 2012, K.E. MacFarlane, M.G. Nordling and P.J. Sack (eds.), Yukon Geological Survey, p. 133-146.

Sawyer, J. and Dickinson, R., 1976. Mount Nansen. *In*: Porphyry Deposits of the Canadian Cordillera, Canadian Institute of Mining and Metallurgy, Special Volume 15, p. 336-343.

Selby, D., Creaser, R.A. and Nesbitt, B.E., 1999. Major and trace element compositions and Sr–Nd–Pb systematics of crystalline rocks from the Dawson Range, Yukon, Canada. Canadian Journal of Earth Sciences, vol. 36, p. 1463-1481.

Smuk, K.A., 1999. Metallogeny of epithermal gold and base metal veins of the southern Dawson Range. Unpublished MSc thesis, McGill University, 155 p.

Smuk, K.A., Williams-Jones, A.E. and Francis, D., 1997. The Carmacks Hydrothermal Event: An Alteration Study in the Southern Dawson Range, Yukon. *In*: Yukon Exploration and Geology 1996, C.F. Roots (ed.), Exploration and Geological Services Division, Indian and Northern Affairs Canada, p. 92-106.

Stevens, R.D., DeLabio, R.N. and Lachance, G.R., 1982. Age determinations and Geological Studies, K-Ar isotopic ages, Report 16. Geological Survey of Canada, Paper 82-2.

Sun, S.S. and McDonough, W.F., 1989. Chemical and isotopic systematics of oceanic basalts: implications for mantle composition and processes. *In*: Magmatism in Ocean Basins, A.D. Saunders and M.J. Norry (eds.), Geological Society of London, Special Publication 42, p. 313-345.

Tafti, R., 2005. Nature, age and origin of Cu-Au mineralization at the Minto and Williams Creek deposits, Yukon. Unpublished MSc thesis, University of British Columbia, 213 p., https://circle.ubc.ca/handle/2429/16627.

Tafti, R., Mortensen, J.K., Lang, J.R., Rebagliati, M. and Oliver, J.L., 2009. Jurassic U-Pb and Re-Os ages for the newly discovered Xietongmen Cu-Au porphyry district, Tibet, PRC: Implications for metallogenic epochs in the southern Gangdese belt. Economic Geology, vol. 104, p. 127-136.

Tempelman-Kluit, D.J., 1979. Transported cataclasite, ophiolite and granodiorite in Yukon: evidence of arc-continent collision. Geological Survey of Canada, Paper 79-14.

Tempelman-Kluit, D.J., 1984. Geology of the Laberge (105E) and Carmacks (115I) map areas. Geological Survey of Canada, Open File 1101, maps with legends, 1:250 000 scale.

Tempelman-Kluit, D.J., 2009. Geology of Carmacks and Laberge map areas, central Yukon: Incomplete draft manuscript on stratigraphy, structure and its early interpretation (*ca.* 1986). Geological Survey of Canada, Open File 5982, 399 p., doi:10.4095/247335.

Walker, G.P.L., 1982. Eruptions of andesitic volcanoes. *In*: Andesites. Orogenic andesites and related rocks, R.S. Thorpe (ed.), John Wiley and Sons, London, p. 403-413.

Wengzynowki, W.A., Giroux, G.H. and Martin, C.J., 2015. NI43-101 Technical Report describing geology, mineralization, geochemical surveys, geophysical surveys, diamond and percussion drilling, metallurgical testing and mineral resources on the Klaza Property. Rockhaven Resources, NI43-101 Technical Report, 173 p. http://www.rockhavenresources.com/assets/projects/2015-06-19_Klaza_NI-43-101.pdf [accessed November 26, 2015].

Wheeler, J.O., 1961. Whitehorse map area, Yukon Territory. Geological Survey of Canada, Memoir 312, 156 p.

Wheeler, J.O. and McFeely, P., 1991. Tectonic assemblage map of the Canadian Cordillera and adjacent parts of the United States of America. Geological Survey of Canada, "A" Series Map 1712A, 2 sheets, doi:10.4095/133549.

Yukon MINFILE, 2007. Yukon MINFILE - A database of mineral occurrences, map 115I - Carmacks (1:250 000), Version 2007-1. Yukon Geological Survey, Energy, Mines and Resources, Yukon Government.

Zagorevski, A., Joyce, N., Ryan, J.J., Roots, C. and Jicha, B., 2014. Middle Cretaceous trimodal Dawson Range magmatism in western Yukon: inferences on sources and tectonic setting (NTS 115I, J and K). Geological Survey of Canada, Open File 7561.

APPENDICES

Appendices are provided as excel spreadsheets.

Appendix 1 U-Pb zircon isotopic analyses and ages

Appendix 2 Whole-rock geochemical analyses

Appendix 3 Sample locations and descriptions